Article

Cell Reports

Galectin-8 Favors the Presentation of Surface-Tethered Antigens by Stabilizing the B Cell Immune Synapse

Graphical Abstract

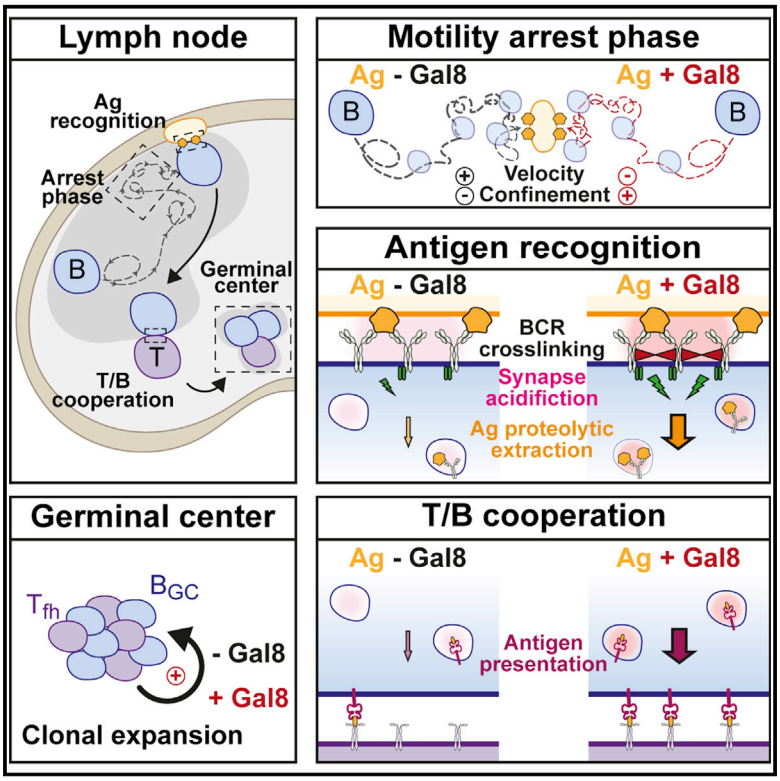

Authors

Dorian Obino, Luc Fetler, Andrea Soza, ..., Marion Espéli, Ana-Maria Lennon-Duménil, Maria-Isabel Yuseff

Correspondence

ana-maria.lennon@curie.fr (A.-M.L.-D.), myuseff@bio.puc.cl (M.-I.Y.)

In Brief

Obino et al. report that Galectin-8 interacts with the BCR, promotes B cell arrest phases during surface-tethered antigen encounter, and facilitates synapse formation and lysosome secretion, which favors the proteolytic extraction of antigens. Consequently, Galectin-8 increases the capacity of B cells to present antigens to helper T cells *in vivo*.

Highlights

- Galectin-8 reinforces B cell arrest phases upon antigen recognition *in vivo*
- Galectin-8 sustains BCR signaling during recognition of immobilized antigens
- This enhances lysosome secretion and favors the proteolytic extraction of antigens
- Galectin-8 improves the capacity of B cells to present antigens to helper T cells

Obino et al., 2018, Cell Reports *25*, 3110–3122
December 11, 2018
https://doi.org/10.1016/j.celrep.2018.11.052

CellPress

OPEN ACCESS
CellPress

Cell Reports
Article

Galectin-8 Favors the Presentation of Surface-Tethered Antigens by Stabilizing the B Cell Immune Synapse

Dorian Obino,[1,10] Luc Fetler,[2,11,12] Andrea Soza,[3,4,12] Odile Malbec,[1] Juan José Saez,[5] Mariana Labarca,[3,4] Claudia Oyanadel,[3,4] Felipe Del Valle Batalla,[5] Nicolas Goles,[5] Aleksandra Chikina,[1,6] Danielle Lankar,[1] Fabián Segovia-Miranda,[5] Camille Garcia,[7] Thibaut Léger,[7] Alfonso Gonzalez,[3,4,8] Marion Espéli,[9] Ana-Maria Lennon-Duménil,[1,13,*] and Maria-Isabel Yuseff[5,13,14,*]

[1]INSERM U932, Institut Curie, Centre de Recherche, PSL Research University, 75248 Paris, Île-de-France, France
[2]CNRS UMR168, Institut Curie, Centre de Recherche, PSL Research University, 75248 Paris, Île-de-France, France
[3]Centro de Biología Celular y Biomedicina (CEBICEM), Facultad de Medicina y Ciencia, Universidad San Sebastián, Santiago, Región Metropolitana 7500961, Chile
[4]Centro de Envejecimiento y Regeneración (CARE), Facultad de Ciencias Biológicas, Pontificia Universidad Católica de Chile, Región Metropolitana, Santiago 8331150, Chile
[5]Departamento de Biologia Celular y Molecular, Facultad de Ciencias Biologicas, Pontificia Universidad Católica de Chile, Region Metropolitana, Santiago 8331150, Chile
[6]CNRS UMR144, Institut Curie, Centre de Recherche, PSL Research University, 75248 Paris, Île-de-France, France
[7]Mass Spectrometry Laboratory, Institut Jacques Monod, UMR 7592, Université Paris Diderot, CNRS, Sorbonne Paris Cite, F-75205 Paris Cedex 13, France
[8]Fundación Ciencia y Vida, Zañartu 1482, Santiago 7750000, Chile
[9]Inflammation, Chimiokines et Immunopathologie, Faculté de Médecine, Université Paris-Sud, INSERM, Université Paris-Saclay, 92140 Clamart, France
[10]Present address: Pathogenesis of Vascular Infections Unit, INSERM U1225, Institut Pasteur, 75015 Paris, France
[11]Present address: CERMES3, INSERM U988, CNRS UMR8211, EHESS, Université Paris Descartes, BP 8, 94801 Villejuif Cedex, France
[12]These authors contributed equally
[13]These authors contributed equally
[14]Lead Contact
*Correspondence: ana-maria.lennon@curie.fr (A.-M.L.-D.), myuseff@bio.puc.cl (M.-I.Y.)
https://doi.org/10.1016/j.celrep.2018.11.052

SUMMARY

Complete activation of B cells relies on their capacity to extract tethered antigens from immune synapses by either exerting mechanical forces or promoting their proteolytic degradation through lysosome secretion. Whether antigen extraction can also be tuned by local cues originating from the lymphoid microenvironment has not been investigated. We here show that the expression of Galectin-8—a glycan-binding protein found in the extracellular milieu, which regulates interactions between cells and matrix proteins—is increased within lymph nodes under inflammatory conditions where it enhances B cell arrest phases upon antigen recognition *in vivo* and promotes synapse formation during BCR recognition of immobilized antigens. Galectin-8 triggers a faster recruitment and secretion of lysosomes toward the B cell-antigen contact site, resulting in efficient extraction of immobilized antigens through a proteolytic mechanism. Thus, extracellular cues can determine how B cells sense and extract tethered antigens and thereby tune B cell responses *in vivo*.

INTRODUCTION

The onset of the adaptive immune response requires the activation of B lymphocytes. This process takes place within lymph nodes and is initiated by the engagement of the B cell receptor (BCR) with antigens tethered at the surface of neighboring cell (Carrasco and Batista, 2007; Junt et al., 2007). This cell-cell contact leads to the formation of an immune synapse where surface-tethered antigens are extracted for further processing and presentation onto major histocompatibility complex class II (MHC-II) molecules at the B cell surface. The B cell synapse is characterized by a central cluster of BCR-antigen complexes surrounded by a ring of integrins that include LFA-1 and VLA-4 (Carrasco and Batista, 2006a; Carrasco et al., 2004). Although synapses can form in the absence of adhesion molecules, the interaction of B cell integrins with ICAM-1 or VCAM enhances contact formation when the avidity for the antigen is low (Carrasco and Batista, 2006b; Carrasco et al., 2004). Thus, the context in which membrane-bound antigens are recognized plays an important role in modulating B cell activation and thus the outcome of B cell responses.

Two non-exclusive mechanisms have been implicated in antigen extraction by B cells. The first one involves the local secretion of lysosomes at the synaptic membrane that release proteases and acidify the synaptic cleft, allowing antigen extraction (Obino et al., 2017; Yuseff et al., 2011). This process relies on

the polarization of the B cell microtubule-organizing center (MTOC) together with MHC-II$^+$/Lamp-1$^+$ lysosomes toward the BCR-antigen interface (Batista et al., 2001; Obino and Lennon-Duménil, 2014; Yuseff et al., 2011). The second one depends on Myosin IIA-mediated pulling forces that trigger invagination of antigen-containing membranes, which are then internalized into clathrin-coated pits (Fleire et al., 2006; Natkanski et al., 2013; Spillane and Tolar, 2017). Interestingly, the mode of antigen extraction used by B cells depends on the physical properties of their environment: antigens presented on flexible surfaces are mechanically internalized, whereas antigens presented on rigid surfaces are taken up through hydrolase secretion. How environmental cues imposed by extracellular matrix (ECM) and ECM-associated proteins regulate antigen extraction remains, however, to be established.

Among the extracellular proteins susceptible of modulating B cell responses to antigens are the proteins from the Galectin family (Rabinovich and Croci, 2012; Rabinovich and Toscano, 2009). They are evolutionarily conserved glycan-binding proteins that, upon secretion, cross-link cell surface glycosylated proteins in the extracellular space (Elola et al., 2015; Kaltner and Gabius, 2012). This property enables them to modulate adhesive interactions between cells and the ECM (Yamamoto et al., 2008), thereby impacting a wide range of processes such as cell growth, apoptosis, and migration (Eshkar Sebban et al., 2007; Hsieh et al., 2008; Lau et al., 2007). Galectins are expressed by most cells of the immune system and are frequently induced upon inflammation (Rabinovich and Toscano, 2009). The production of Galectin-1 and -8 is significantly upregulated by activated T and B cells, macrophages, and natural killer (NK) cells, and both Galectins have redundant roles in promoting plasma cell formation (Rabinovich and Croci, 2012; Tsai et al., 2011). In addition, Galectin-8 has been implicated in autoimmune diseases such as systemic lupus erythematosus (SLE) and multiple sclerosis where function-blocking autoantibodies against Galectin-8 are frequently detected (Eshkar Sebban et al., 2007; Massardo et al., 2009; Pardo et al., 2017). These observations suggest that Galectin-8 is a good candidate for the modulation of B cell activation in tissues.

We here show that Galectin-8 is expressed at the subcapsular sinus where B cells recognize surface-tethered antigens and that it enhances B cell responses *in vivo*. This effect results from the ability of extracellular Galectin-8 to (1) reinforce B cell arrest phases upon antigen recognition *in vivo*, (2) promote synapse formation during BCR recognition of tethered antigens by triggering a faster recruitment and secretion of lysosomes toward the B cell-antigen contact site, and (3) strengthen B cell activation by enhancing BCR downstream signaling through the phosphoinositide 3-kinase (PI3K) pathway. These results highlight a key role for Galectin-8 in modulating B cell responses and provide insights on how extracellular cues can tune the ability of B cells to respond to surface-tethered antigens *in vivo*.

RESULTS

Galectin-8 Is Highly Expressed in the Sub-capsular Sinus of Lymph Nodes

We analyzed the distribution of Galectin-8 in lymphoid tissues. *Lgals8* mRNA was found in mouse bone marrow, spleen, and lymph nodes at steady state (Figure 1A), consistent with a previous report (Tribulatti et al., 2009). Additionally, we observed that, within lymph nodes, Galectin-8 was highly expressed at the level of the sub-capsular sinus (SCS) (Figure 1B). Remarkably, *Lgals8* mRNA levels were upregulated in lymph nodes from mice with systemic exposure to lipopolysaccharide (LPS) (Figure S1A). Under these conditions, expression of Galectin-8, detected by β-galactosidase activity under the promoter of the *Lgals8* gene, displayed a more diffused expression pattern at the cortex of lymph nodes and particularly within the paracortical area where T cells reside (Figure S1B). However, under steady-state conditions, co-localization studies showed that, at the level of the SCS, Galectin-8 was highly expressed where both B cells and SCS CD169$^+$ macrophages sit (Figure 1C). SCS macrophages have been described as retaining particulate antigens at their surface for presentation to follicular B cells (Carrasco and Batista, 2007; Junt et al., 2007). Of note, while no association between Galectin-8 localization and T cells was observed in the lymph node medulla, Galectin-8 was intensely expressed within the vasculature (Figure S1C). These results highlight that Galectin-8 is expressed within the lymph node regions where B cells acquire and process cell-surface tethered antigens.

Galectin-8 Enhances the Arrest Phases of B Cells *In Vivo*

We thus investigated whether addition of extracellular Galectin-8 modulates the capacity of B lymphocytes to extract antigens tethered at the surface of SCS macrophages. We preferred this strategy to knocking out Galectin-8 gene as this c-type lectin was shown to have a redundant role with another member of the Galectin family, Galectin-1, upon plasma cell differentiation (Tsai et al., 2011). Thus, defects associated to Galectin-8 deficiency should most likely be compensated by Galectin-1 *in vivo*. To address the role of Galectin-8 in antigen extraction by B cells, we adoptively transferred HEL-specific spleen B cells from MD4 transgenic mice (Goodnow et al., 1988) expressing fluorescent MHC-II molecules (MHC-II-GFP) (Boes et al., 2002) into wild-type (WT) (C57BL/6) recipients, which were then immunized 16 hr later by footpad injection of fluorescent microspheres coated with HEL plus Galectin-8 or BSA as control (coated with equal antigen amounts; Figure 2A). Antigen-coated beads were deposited at the surface of SCS macrophages as previously reported (Carrasco and Batista, 2007), and no difference in their distribution was observed between the various experimental conditions (Figure 2B).

Intra-vital imaging of the draining popliteal lymph node was performed 30 min post-immunization. Tracking of HEL-specific B cells (green, MHC-II-GFP) present within the upper part of the draining lymph node (Figure 2B; Video S1) showed that they displayed shorter and more confined trajectories upon HEL-BSA exposure than naive (no antigen) and antigen non-specific B cells (Figures 2C–2E). In addition, HEL-specific B cells showed reduced mean cell velocity after antigen administration (Figure 2F) and the percentage of time they spent at low speed (<1 μm/min) increased (Figure 2G; 19% for naive B cells versus 37% for HEL-BSA-stimulated B cells). These results are consistent with previous reports highlighting that antigen recognition triggers an arrest phase in B cell migration, thereby allowing the acquisition of cell-surface tethered antigens (Carrasco and

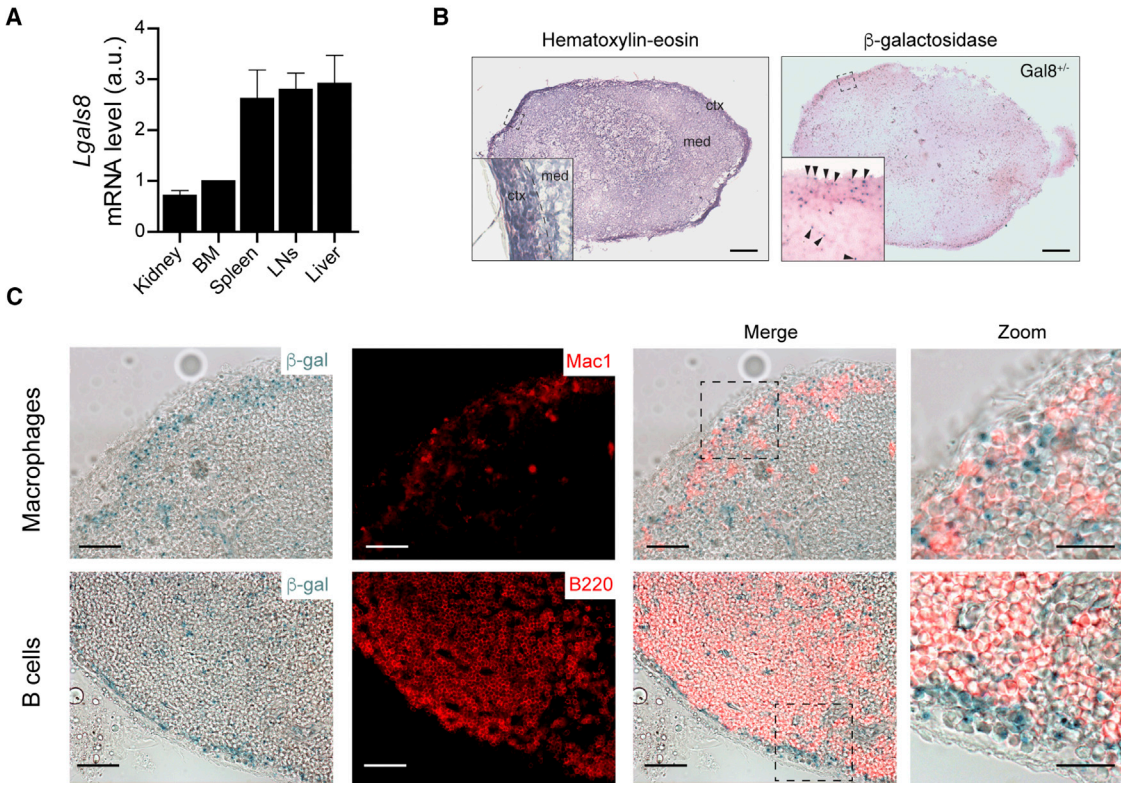

Figure 1. Galectin-8 Is Expressed in Lymphoid Tissues

(A) qRT-PCR analysis of Galectin-8 (*Lgals8*) mRNA levels in kidney, bone marrow (BM), spleen, lymph nodes (LNs), and liver of C56BL/6 WT mice. Values were normalized with respect to the BM condition for each mouse. n = 5 mice pooled from N = 3 independent experiments. Bar graphs indicate mean ± SEM.

(B) Representative images of H&E staining (left) and β-galactosidase staining (right) of LN cryosection from heterozygous mouse bearing a LacZ expression cassette on one allele of the *Lgals8* locus. Arrowheads on the inset highlight β-galactosidase staining within the SCS area. Scale bar, 150 μm.

(C) Representative images of serial lymph node cryosections stained for β-galactosidase (Galectin-8) and macrophages (Mac1) or B cells (B220). Scale bar, 200 μm. Zooms highlight the spatial localization of Galectin-8 together with macrophages and B cells at the SCS. Scale bar, 30 μm.

See also Figure S1.

Batista, 2007; Junt et al., 2007). Strikingly, track length and mean B cell velocity were even more drastically reduced when antigen was administered together with Galectin-8 (Figures 2C–2F). Accordingly, in this condition, B cells remained at low speed for prolonged periods when compared to B cells exposed to HEL-BSA (Figure 2G; 37% for HEL-BSA versus 51% for HEL-Galectin-8 [Gal8]). Importantly, in the absence of BCR engagement with specific antigens, Galectin-8 had no effect on the migratory behavior of B cells (Figures 2F–2H). These data strongly suggest that extracellular Galectin-8 enhances the arrest phase during which B cells extract antigens *in vivo*.

Galectin-8 Enhances Particulate-Antigen Acquisition by B Cells *In Vivo*

We next assessed whether the enhanced arrest phase observed in B cells upon exposure to antigens plus extracellular Galectin-8 translated into an increased capacity to acquire particulate antigens *in vivo*. To this end, as described above, carboxyfluorescein succinimidyl ester (CFSE)-labeled HEL-specific spleen B cells were adoptively transferred into WT recipient mice, and 24 hr later, recipient mice were immunized by footpad injection of HEL ± Galectin-8-coated microspheres. We then monitored the percentage of HEL-specific B cells (green) loaded with particulate antigens (red) at 16 hr post-immunization by imaging popliteal lymph node cryosections (Figure 3A). In agreement with the data presented above, exposure of HEL-specific B cells to HEL-Galectin-8 increased their capacity to internalize particulate antigens when compared to HEL-specific B cells exposed to HEL-BSA microspheres (Figure 3B). We next determined the number of antigen-loaded microspheres associated with individual HEL-specific B cells (Figure 3C). While the proportion of HEL-specific B cells loaded with only one microsphere decreased when exposed to HEL-Galectin-8 (77%) compared to HEL-BSA (53%), the proportion of cells that accumulated more than five microspheres greatly increased (0% versus 22%, respectively; Figure 3D). Altogether, these results strongly support a role for extracellular Galectin-8 in favoring particulate antigen acquisition by antigen-specific B cells by enhancing their arrest phase *in vivo*.

Galectin-8 Stimulates T-B Cooperation *In Vivo*

We then questioned the physiological relevance of these findings by investigating whether extracellular Galectin-8 promotes B cell dependent activation of $CD4^+$ T lymphocytes *in vivo*. Antigen

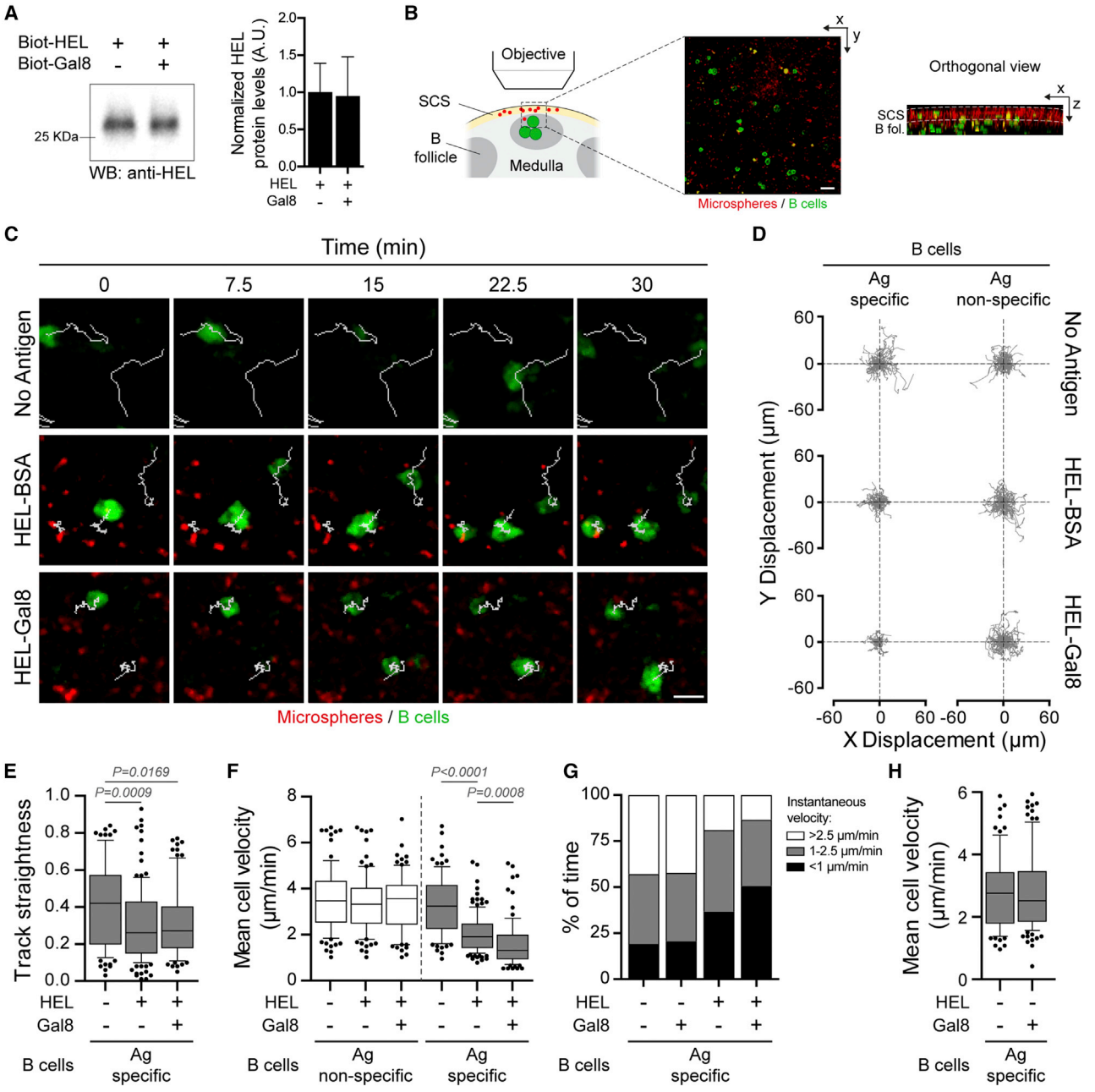

Figure 2. Galectin-8 Promotes B Cell Arrest Phases *In Vivo*

(A) Representative western blot and quantification of the amounts of antigen (HEL) effectively immobilized at the surface of 0.2-µm microspheres in the presence of Galectin-8 or not. Data are pooled from N = 3 independent experiments. Bar graphs indicate mean ± SEM.

(B) Schematic and representative image of the observed area within draining popliteal lymph nodes (pLN). Scale bar, 20 µm. The orthogonal view shows the deposit of microspheres at the periphery of pLN.

(C) Representative images of HEL-specific migrating B cells (green) within the sub-capsular area of lymph nodes upon immunization with indicated microspheres (red). Scale bar, 8 µm.

(D) Relative tracks of HEL-specific (MD4) and non-specific (WT) B cells.

(E) Track straightness of B cells shown in (C). Boxes extend from the 25th to 75th percentile, with a line at the median and whiskers extend from the 10th to the 90th percentile.

(F) Mean cell velocity of HEL-specific (gray) and non-specific (white) B cells upon immunization with indicated microspheres. Boxes extend from the 25th to 75th percentile, with a line at the median and whiskers extend from the 10th to the 90th percentile.

(G) Quantification of the percentage of time cells spent at high (>2.5 µm/min; white), intermediate (between 1 and 2 µm/min; gray), and very slow (<1 µm/min; black) speed.

(legend continued on next page)

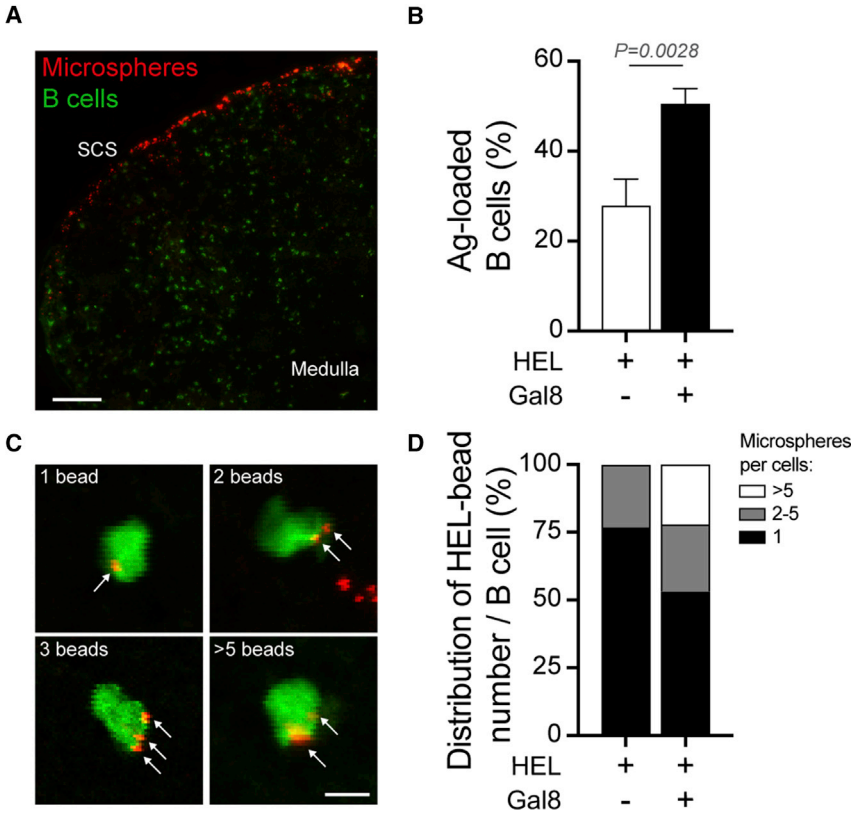

Figure 3. Galectin-8 Promotes Particulate-Antigen Acquisition *In Vivo*

(A) Representative image of popliteal lymph node cryosection from recipient mice, showing the distribution of HEL-coated (in absence of Galectin-8) microspheres (red) within the sub-capsular area and adoptively transferred Ag-specific B cells (green). Scale bar, 150 μm.

(B) Quantification of the percentage of HEL-specific B cells loaded with HEL-coated microspheres in combination or not with Galectin-8. n > 100 cells pooled from N = 2 mice per condition. Unpaired t test was used to assess statistical significance. Bar graphs indicate mean ± SEM.

(C) Representative images showing the internalization and accumulation of Ag-coated microspheres within Ag-specific B cells. Scale bar, 8 μm.

(D) Distribution of the number of Ag-coated microspheres per B cells analyzed in (B).

presentation to CD4$^+$ T lymphocytes induces the formation of germinal centers (GCs) characterized by the emergence of GC B cells (B220$^+$GL7$^+$FAS$^+$) and follicular helper T cells (Tfh) (CD4$^+$CXCR5$^+$PD-1$^+$) (De Silva and Klein, 2015). For this reason, adoptive cell transfer experiments (donors: HEL-specific B cells from SW_{HEL} transgenic mice [Phan et al., 2003] and ovalbumin [OVA]-specific CD4$^+$ T cells from OT-II transgenic mice, both CD45.2; recipients: C57BL/6, CD45.1) were performed to monitor the generation of GC B and Tfh cells 8 days post-immunization (Figure 4A). We found that the presence of extracellular Galectin-8 enhanced the presentation of immobilized antigens as revealed by the higher numbers of both GC B and Tfh cells found in mice immunized with HEL/OVA plus Galectin-8 compared to mice immunized with only HEL/OVA (Figures 4B–4E). Importantly, equal amounts of HEL were immobilized at the surface of beads under the different conditions used (Figure 4A), and as previously observed, in absence of specific BCR ligand, Galectin-8 was not able to induce the generation of GC B and Tfh cells (Figures 4D and 4E). Importantly, mouse immunization with OVA/Galectin-8 only—i.e., in absence of the B cell antigen HEL—no GC B cells and few Tfh cells were detected (Figures 4D and 4E), supporting a role for extracellular Galectin-8 directly on B cells rather than T cells.

However, because these experiments were conducted in WT recipient mice expressing endogenous Galectin-8, we could not formally show that extracellular exogenous Galectin-8 was solely responsible for the enhanced antigen presentation capacity observed *in vivo*. To address this issue, we repeated the mouse immunization experiments described above using *Lgals8*$^{-/-}$ recipient mice (Figure 4A). Under these conditions, Galectin-8 expression was abolished in recipient mice, which therefore allowed us to determine the specific contribution of extracellular Galectin-8 in tuning B cell antigen presentation capacity. Strikingly, immunization of *Lgals8*$^{-/-}$ recipient mice with HEL/OVA led to an impaired generation of GC B and Tfh cells when compared to *Lgals8*$^{+/+}$ control counterparts (Figures 4F and 4G), strongly arguing for a role of extracellular Galectin-8 in enhancing antigen presentation by B cells. Importantly, immunization of these mice with HEL/OVA plus exogenous Galectin-8 partially rescued the antigen presentation capacity of HEL-specific B cells as revealed by the numbers of GC B and Tfh cells (Figures 4F and 4G). Hence, extracellular Galectin-8 enhances the capacity of antigen-specific B cells to extract and present immobilized antigens to CD4$^+$ T cells and enter the GC reaction *in vivo*.

Galectin-8 Favors Immobilized-Antigen Extraction and Presentation *In Vitro*

We next searched for a mechanism by which Galectin-8 promotes antigen extraction by B cells. We first confirmed the effect of Galectin-8 in enhancing the capacity of B cells to extract and present immobilized antigens to CD4$^+$ T cells *in vitro* using standardized experimental setups, as previously described (Yuseff

(H) Mean cell velocity of HEL-specific B cells upon immunization with microspheres coated with non-relevant antigen (BSA) in combination or not with Galectin-8. Boxes extend from the 25th to 75th percentile, with a line at the median and whiskers extend from the 10th to the 90th percentile.

In (D)–(H), n > 80 cells from 4 mice per condition pooled from N = 4 independent experiments. Kruskal-Wallis test was used to assess statistical significance. See also Video S1.

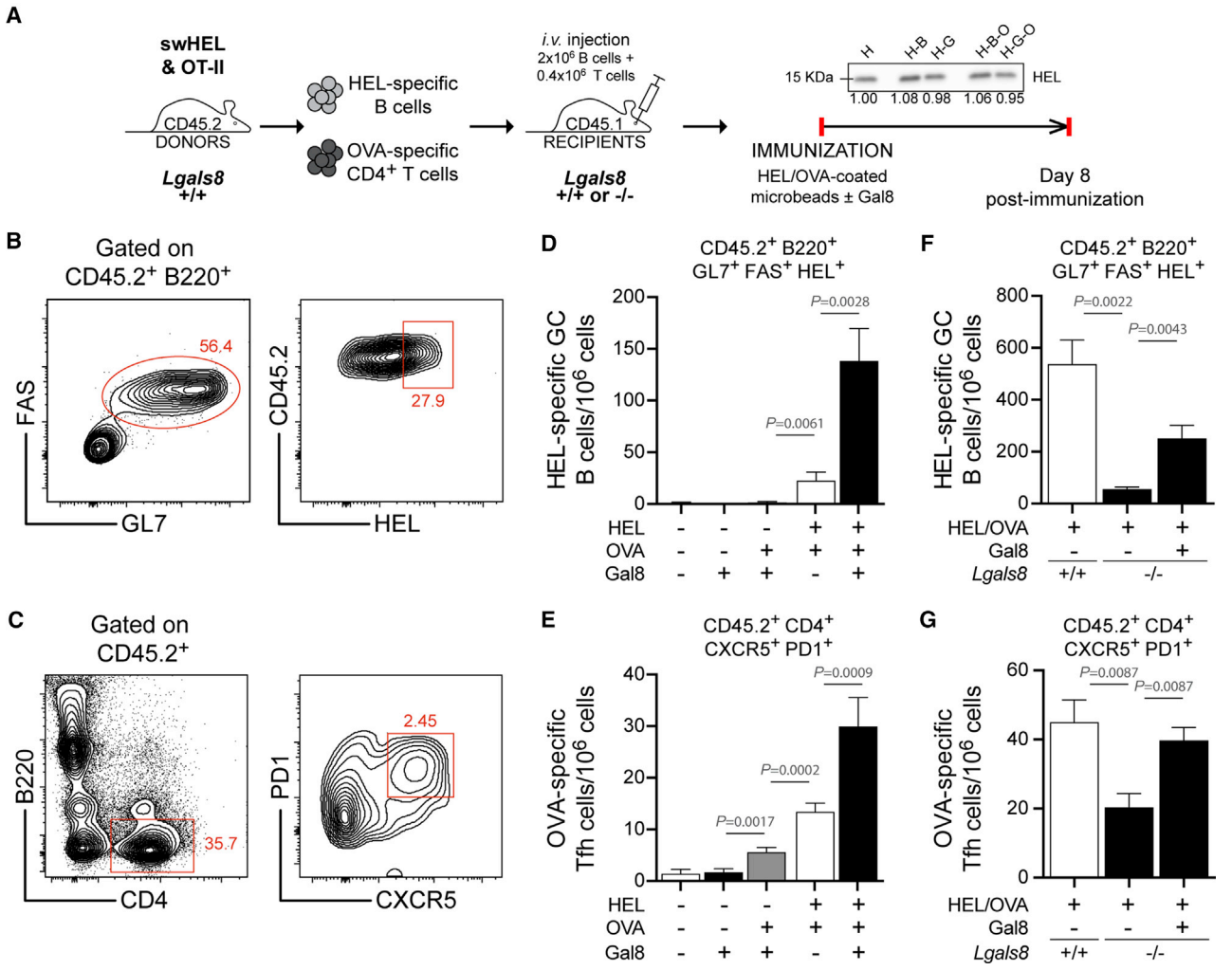

Figure 4. Exogenous Galectin-8 Favors T-B Cooperation *In Vivo*

(A) Schematic of the experimental approach used to assess the ability of B cells to present antigen to CD4$^+$ T cells *in vivo*. The western blot shows the amounts of antigen (HEL) effectively immobilized at the surface of 0.2-μm microspheres in the different conditions used to immunize mice. H, HEL alone; H-B, HEL-BSA; H-G, HEL-Galectin-8; H-B-O, HEL-BSA-OVA; H-G-O, HEL-Galectin-8-OVA. Numbers below the blot represent the normalized density of the bands with respect to the HEL alone condition. Data are representative of N = 3 independent experiments.

(B and C) Representative dot plots used for the gating of (B) HEL-specific GC B cells (CD45.2$^+$B220$^+$HEL$^+$GL7$^+$FAS$^+$) and (C) OVA-specific OT-II Tfh cells (CD45.2$^+$CD4$^+$CXCR5$^+$PD1$^+$).

(D and E) Quantification of the number of (D) HEL-specific GC B cells and (E) OVA-specific OT-II Tfh cells following mouse immunization with indicated microspheres. n = 10 mice per condition pooled from N = 3 independent experiments.

(F and G) Quantification of the number of (F) HEL-specific GC B cells and (G) OVA-specific OT-II Tfh cells in CD45.1 *Lgals8*$^{+/+}$ or *Lgals8*$^{-/-}$ recipient mice (adoptively transferred with CD45.2 *Lgals8*$^{+/+}$ SW$_{HEL}$ B cells and OT-II CD4$^+$ T cells) following their immunization with indicated microspheres. n = 6 mice per condition pooled from N = 2 independent experiments. Kruskal-Wallis test was used to assess statistical significance. All bar graphs indicate mean ± SEM.

and Lennon-Dumenil, 2013; Yuseff et al., 2011) (see STAR Methods for details). As expected from our *in vivo* results, both antigen extraction and presentation were enhanced upon stimulation of primary spleen B cells with BCR-ligand$^+$ beads coated with Galectin-8 (Figures 5A and 5B). Similar results were obtained when stimulating the B lymphoma model cell line IIA1.6 (Figure S2). Strikingly, the amount of antigen extracted at early time points was significantly higher when Galectin-8 was present (Figures 5A, S2A, and S2B). After 120 min, the total amount of antigen extracted reached a plateau and was equal in both conditions (Figures 5A, S2A, and S2B). Importantly, in the absence of BCR engagement with specific antigens, Galectin-8 did not trigger antigen extraction by B cells (Figure S2C).

Consistent with these results, the processing and presentation of antigens, as revealed by the secretion of interleukin-2 (IL-2) by T cells, was significantly higher in the presence of Galectin-8 both in primary B cells and in the B cell line (Figures 5B and S2D). Peptide presentation showed no major differences

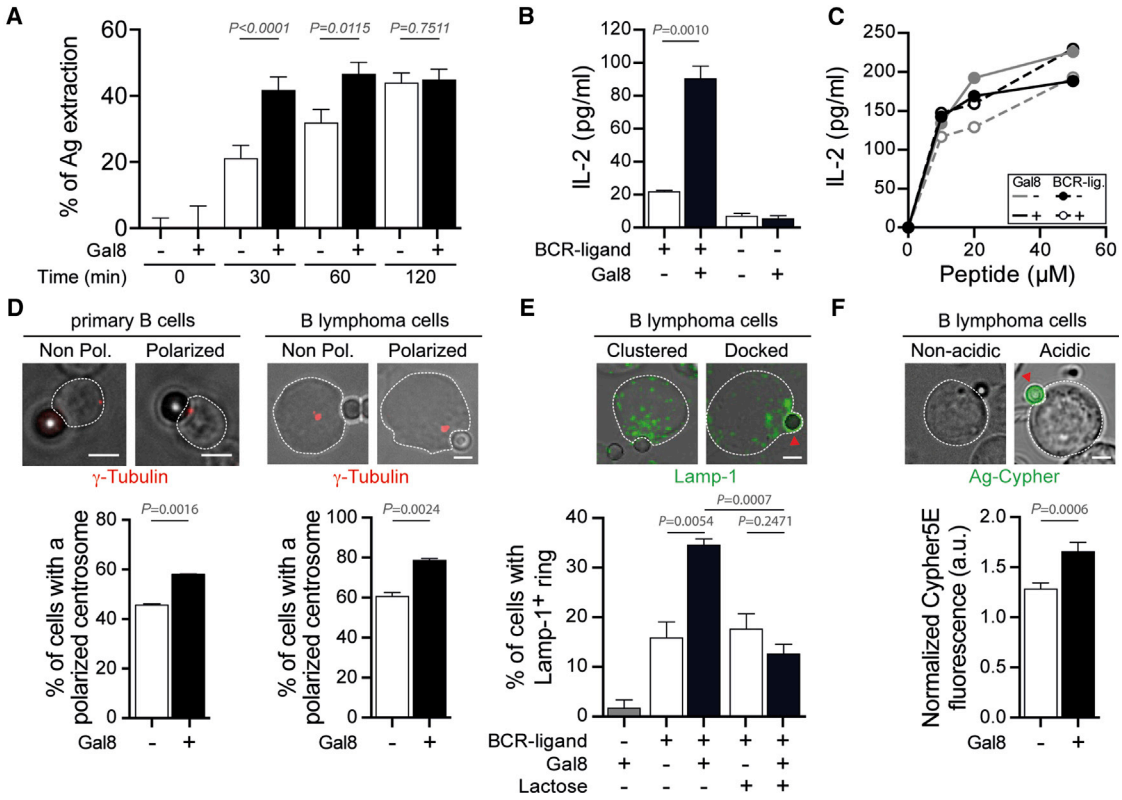

Figure 5. Extracellular Galectin-8 Favors Lysosome Secretion at the B Cell Synapse

(A) Quantification of the percentage of antigen (OVA) extracted from beads following incubation of primary spleen B cells with indicated beads and time. Values were normalized with respect to Ag-coated beads not engaged with B cells. n > 60 cells pooled from N = 2 independent experiments. Unpaired t test was used to assess statistical significance. Bar graphs indicate mean ± SEM.

(B) Antigen (*Lack*) presentation assay with spleen B cells in presence or not of exogenous Galectin-8. Bars show the mean ± SEM of triplicate and are representative of N = 2 independent experiments. Unpaired t test was used to assess statistical significance.

(C) Peptide controls for cells used in the antigen presentation assays shown in (B). Graph shows the mean of duplicates and is representative of N = 2 independent experiments.

(D) Representative images of non-polarized and polarized centrosomes (γ-Tubulin) in primary B cells (left) and a B lymphoma cell line (right). Scale bar, 3 μm. The lower panel shows the quantification of the percentage of cells having polarized their centrosome following 60-min stimulation with BCR-ligand$^+$ beads containing or not Galectin-8. Paired t test was used to assess statistical significance. Bar graphs indicate mean ± SEM. n > 50 cell/bead conjugates assessed per condition pooled from N = 2 independent experiments (primary B cells) and N = 3 independent experiments (B cell line).

(E) Representative images of B cells harboring the characteristic Lamp-1$^+$ ring of lysosomes docked at the cell-bead interface. Scale bar, 3 μm. The lower panel shows the quantification of the percentage of cells displaying Lamp-1$^+$ rings upon stimulation with BCR-ligand$^+$ beads containing or not Galectin-8 and in presence or not of 100 mM lactose for 60 min. n > 60 cell/bead conjugates assessed per condition pooled from N = 3 independent experiments. Kruskal-Wallis test was used to assess statistical significance. Bar graphs indicate mean ± SEM.

(F) Representative images of B cells harboring acidic synapse as revealed by the appearance of Cypher5E fluorescence on the BCR-ligand$^+$ bead. Scale bar, 3 μm. The lower panel shows the quantification of the Cypher5E fluorescence intensity in cell-bead conjugates following a 90-min stimulation with BCR-ligand$^+$ beads containing or not Galectin-8. Values were normalized with respect to the mean fluorescence intensity of beads that were not engaged in immune synapses. n > 270 cell/bead conjugates assessed per condition pooled from N = 2 independent experiments.

See also Figures S2, S3, and S4.

between both conditions (Figures 5C and S2E), indicating that Galectin-8 does not affect cell surface levels of MHC-II molecules and does not influence B-T cell interactions per se. Importantly, in the presence of lactose, which inhibits Galectin binding, the effect of Galectin-8 was blocked, and the levels of antigen presentation were comparable to control conditions where Galectin-8 is absent (Figures S2D and S2E). Altogether, our results show that Galectin-8 also stimulates the capacity of B cells to extract and present immobilized antigens to CD4$^+$ T cells *in vitro*.

Galectin-8 Enhances the Proteolytic Extraction of Immobilized Antigens at the B Cell Synapse

Two mechanisms have been proposed to promote the extraction of tethered antigens by B cells. While the first one involves B cell polarization and lysosome secretion within the synaptic cleft allowing the proteolytic extraction of the tethered antigens (Obino et al., 2017; Yuseff et al., 2011), the second one relies on cycles of B cell spreading and contraction coupled to mechanical extraction through pulling forces exerted by the motor protein Myosin II (Fleire et al., 2006; Harwood and Batista, 2011;

Natkanski et al., 2013). To determine which pathway was affected by Galectin-8, we first evaluated the ability of this lectin to induce B cell spreading. To this end, B cells were seeded on poly-L-lysine (PLL)- or Galectin-8-coated coverslips, and their spreading area was monitored over time (Figure S3A). Strikingly, surface-immobilized Galectin-8 strongly enhanced B cell spreading (Figure S3B) and promoted the formation of actin protrusions, suggesting that this glycan-binding protein may strengthen cycles of actin-dependent cell spreading and contraction. Of note, B cells seeded on substrates containing Galectin-8 pretreated with lactose did not display a strong spreading response (Figures S3C and S3D). We confirmed that lactose blocked the interaction of this lectin with B cells by showing that pre-treatment of soluble recombinant Galectin-8 with lactose or thiodigalactoside (TDG) (another specific inhibitor of Galectin glycan binding sites) prevents Galectin-8 binding to the B cell surface (Figure S3E). Despite the effects observed on actin cytoskeleton remodeling, stimulation of B cells in the presence of Galectin-8 did not trigger higher levels of myosin regulatory light chain (MLC) phosphorylation, an indicator of Myosin II activation (Figure S3F), suggesting that proteolytic rather than mechanical extraction of antigens is being reinforced under these conditions.

Accordingly, when stimulated in the presence of extracellular Galectin-8, a higher proportion of B cells showed polarized centrosomes (Figure 5D). Analogous observations were made in a B lymphoma cell line, which was further used to study lysosome docking and polarity, because of their larger size. Indeed, enhanced recruitment and docking of lysosomes at the antigen-contact site was observed in the presence of Galectin-8, compared to cells stimulated with BCR ligands alone (Figure 5E). Of note, addition of lactose during B cell stimulation blocked the effect of Galectin-8, and the proportion of B cells with docked lysosomes at the immune synapse was comparable to control conditions where Galectin-8 is absent (Figure 5E). Consistent with these data, we observed that Galectin-8 stimulates the acidification of the B cell synapse as measured using beads coated with antigens coupled to the pH-sensitive dye Cypher5E (Figure 5F). Hence, Galectin-8 promotes the proteolytic extraction of bead-associated antigens by facilitating B cell polarization, lysosome recruitment, and secretion at the B cell synapse. Importantly, we further found that B cells lacking endogenous Galectin-8 expression normally polarized their centrosome and lysosomes to the immune synapse (Figure S4A) and only displayed a minor delay in their capacity to extract immobilized antigens (Figure S4B). In agreement with our *in vivo* data, these results argue for a role of Galectin-8 in the extracellular environment rather than a B cell-intrinsic function of this glycan-binding protein in its ability to enhance B cell responses.

Galectin-8 Enhances B Cell Functions by Interacting with the BCR

Finally, we searched for the B cell surface partner(s) of extracellular Galectin-8. To this end, GST-pull-down experiments and mass spectrometry analyses were conducted to identify Galectin-8 interacting proteins present within spleen B cell lysates. In agreement with previous studies showing that Galectin-8 interacts with the integrin LFA-1 (Cárcamo et al., 2006; Diskin et al., 2009; Vicuña et al., 2013), we found that both LFA-1 subunits, alpha-L and beta-2 (also known as CD11a and CD18, respectively), were present among the top hits (Table S1, red). Of note, proteins belonging to the B cell antigen BCR complex itself (Table S1, blue) as well as members of the Galectin family, Galectin-9 and the bait protein Galectin-8 (Table S1, green), were also found. The integrin LFA-1 represented an interesting candidate since it was described to promote B cell spreading but also, when engaged with its counter-receptor ICAM-1, decreases the threshold for BCR activation when antigen avidity is low (Carrasco et al., 2004; Saez de Guinoa et al., 2013). However, when repeating the Galectin-8 GST-pull-down assay and performing immunoblot experiments for this integrin, we were not able to confirm the interaction between LFA-1 and Galectin-8 in B cells (Figure 6A). In agreement with this result, pre-treatment of B cells with function-blocking antibodies against LFA-1 did not impair the extensive spreading observed when B cells are plated onto Galectin-8-coated surfaces (Figure 6B), nor the cell surface binding of soluble Galectin-8 (Figure 6C). Therefore, it is unlikely that the observed effects of Galectin-8 on B cell functions result from an interaction of this glycan-binding protein with surface LFA-1.

We next investigated a potential interaction of Galectin-8 with the BCR itself. The interaction between both proteins was confirmed by pull-down assays, where we found that GST-Galectin-8 formed a complex with the BCR (Figure 6D). Of note, this interaction was inhibited by the addition of lactose showing the glycan-specificity of the interaction (Figure 6D, lactose +). Given that the BCR controls both antigen uptake and elicits downstream signaling upon ligand engagement, we evaluated whether Galectin-8 regulates BCR downstream signaling pathways. Our results show that while Galectin-8 barely affected Syk and ERK signaling, it enhanced the phosphorylation of Blnk, Btk, and Akt, which were higher and more sustained in time (Figure 6E). Interestingly, Btk and Akt signaling molecules are part of the PI3K pathway involved in the determination of B cell activation and fate upon antigen encounter (Limon and Fruman, 2012). Alternatively, the Akt signaling pathway has also been described to regulate antigen presentation by macrophages and dendritic cells through the mammalian target of rapamycin (mTOR)-dependent regulation of the lysosomal activity (Saric et al., 2016). Altogether, these results suggest that Galectin-8 was unlikely enhancing antigen extraction and presentation by modulating integrin activity but rather by directly modulating the signaling properties of the BCR upon particulate-antigen encounter.

DISCUSSION

We here show that Galectin-8 is expressed in the SCS and promotes antigen extraction and presentation by B lymphocytes, reinforcing the cooperation between T and B cells *in vivo*. We further highlight using quantitative *in vitro* assays that this effect of Galectin-8 is mediated at least in part by (1) interacting directly with the BCR to strengthen downstream signaling via the PI3K pathway and (2) enhancing the recruitment and secretion of lysosomes at the B cell synapse. Higher antigen extraction translates into longer phases of interaction between B cells and antigen presenting cells in the B cell follicle as highlighted by intra-vital

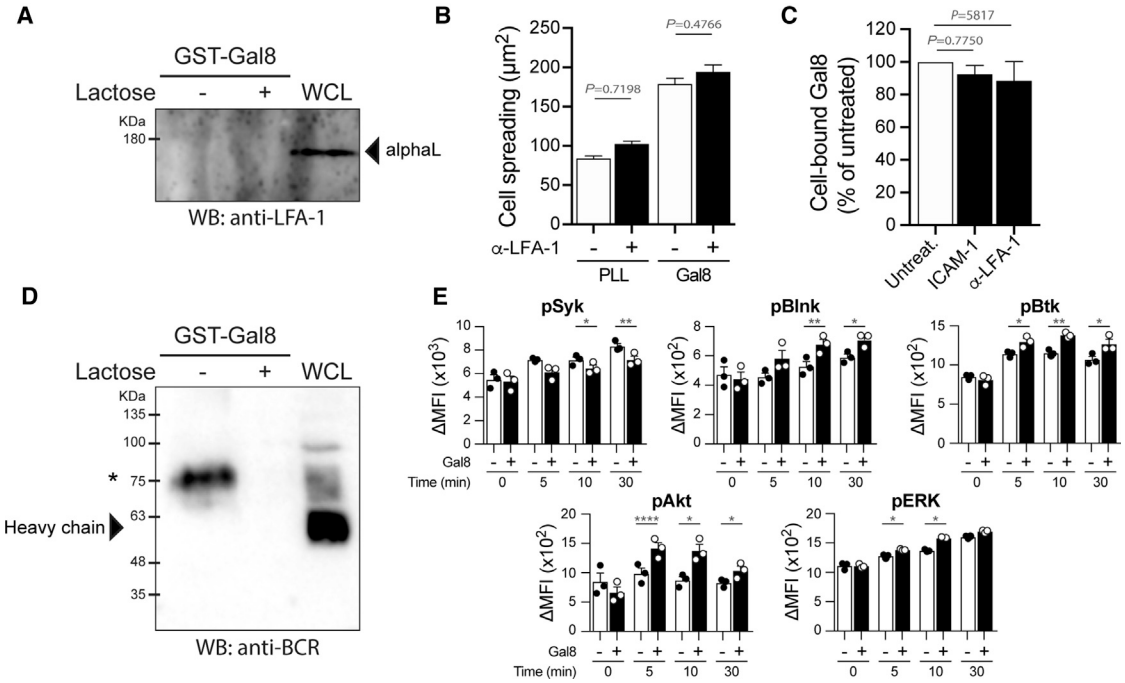

Figure 6. Galectin-8 Interacts with the BCR

(A) GST-Galectin-8 pull-down experiments highlighting the absence of interaction between Galectin-8 and LFA-1 (lanes 1 and 2). Lane 3 shows the detection of LFA-1 in the whole-cell lysate (WCL). Representative of N = 4 independent experiments.

(B) Quantification of the spreading area of B cells pre-treated or not for 30 min with 10 μg/mL function-blocking anti-LFA-1 antibody and seeded on poly-L-lysine (PLL)- or Galectin-8-coated coverslips. n > 60 cells per condition pooled from N = 3 independent experiments. ANOVA test followed by a Sidak's multiple-comparison test was used to assess statistical significance. Bar graphs indicate mean ± SEM.

(C) Flow cytometry quantification of cell-bound Alexa Fluor 488-conjugated Galectin-8 following a 60-min incubation with B cells pre-treated or not for 30 min with 2 μg/mL recombinant ICAM-1 or 10 μg/mL function-blocking anti-LFA-1 antibody. Values were normalized with respect to the untreated condition in each experimental replicate. Data are pooled from N = 2 independent experiments. ANOVA test followed by a Sidak's multiple-comparison test was used to assess statistical significance. Bar graphs indicate mean ± SEM.

(D) GST-Galectin-8 pulls down the BCR from B cell extracts (lane 1), which is inhibited in presence of 100 mM lactose (lane 2), indicating the dependency of Galectin-8/glycan interactions. Lane 3 shows the detection of the BCR in the whole-cell lysate (WCL). *The higher molecular weight could correspond to a highly glycosylated form of the BCR or a stable complex between the Ig heavy and light chain. Representative of N = 3 independent experiments.

(E) Flow cytometry analysis of the phosphorylation status of BCR-downstream signaling molecules upon stimulation of primary spleen B cells with BCR-ligand$^+$ beads containing or not Galectin-8 for indicated times. Values were normalized with respect to the non-stimulated condition for each mouse. Each dot on the bar graphs corresponds to cells purified from independent mice. Data are representative of N = 2 independent experiments. Ratio t test was used to assess statistical significance. *p < 0.05; **p < 0.01; ****p < 0.0001. Bar graphs indicate mean ± SEM.

See also Table S1.

microscopy. Galectin-8 therefore emerges as an ECM-associated protein that acts as an extracellular cue to stimulate B cell responses to T cell-dependent antigens *in vivo*.

Galectins are considered part of the environmental stimuli that shape immune responses depending on their local concentration and glycosylated ligands exposed on the surface of immune cells (Rabinovich and Croci, 2012; Rabinovich and Toscano, 2009). Interestingly, during differentiation and/or activation, immune cells can change the glycosylation patterns of their receptors and thereby modulate interactions with specific Galectins (Marth and Grewal, 2008). Galectin-1 and -8 were both shown to promote the differentiation of LPS-treated B cells into antibody-secreting plasma cells (Anginot et al., 2013; Tsai et al., 2008, 2011). Whereas higher concentrations of Galectin-8 trigger antigen-independent CD4$^+$ T cell proliferation, lower concentrations of this lectin act as a co-stimulatory signal that favors antigen-specific CD4$^+$ T cell responses (Cattaneo et al., 2011; Tribulatti et al., 2009). We found that, under inflammatory conditions, the expression of Galectin-8 increased significantly within lymph nodes. However, due to the lack of specific antibodies, we could not determine which specific cell types were producing Galectin-8. Interestingly, lymph node-resident cells, such as lymphatic endothelial cells, express Podoplanin, a transmembrane glycoprotein, recently described to interact with Galectin-8 (Cueni and Detmar, 2009). Thus, along with detecting the cell types that produce Galectin-8, it would be important to study receptors located at the surface of antigen-presenting cells, which could immobilize Galectin-8 at their cell surface to modulate their effector functions. Additionally, changes in glycosylation patterns at the surface of B cells, generated by LPS treatment, could equally contribute to enhance interactions with Galectin-8. Moreover, the immunoregulatory effects of

Galectins are frequently altered under pathological conditions such as autoimmunity (Pardo et al., 2017; Sarter et al., 2013). The sera of patients suffering from SLE or multiple sclerosis contain autoantibodies with functional blocking activity against Galectin-8 (Cárcamo et al., 2006; Massardo et al., 2009; Pardo et al., 2017; Vicuña et al., 2013), suggesting that this lectin could play a role in B cell homeostasis and function. However, the impact of Galectin-8 in regulating antigen presentation and B cell responses *in vivo* had not been explored until now.

The tight coupling between arrests in cell motility and the establishment of a stable immune synapse is critical for B cells to efficiently extract and process antigens *in vivo*. We provide evidence for the role of Galectin-8 in both processes and reveal potential mechanisms involved. We show that Galectin-8 triggers the formation of actin protrusions and extensive cell spreading in B cells, which could favor the formation of a stable immune synapse. Indeed, cortical actin cytoskeleton remodeling plays a key role in regulating the adhesive properties of B cells at the site of antigen encounter by promoting a spreading response and controlling receptor signaling (Mattila et al., 2016). Additionally, actin-binding proteins, such as Vinculin, can stabilize LFA-1 at the synaptic membrane and strengthen the adhesive capacity of B cells (Saez de Guinoa et al., 2013). Galectin-8 was shown to bind to LFA-1 in T cells and to promote actin rearrangements by activating Rho and Rac signaling pathways (Cárcamo et al., 2006; Diskin et al., 2009; Vicuña et al., 2013). However, our data reveal that the effect of Galectin-8 on actin cytoskeleton remodeling does not rely on its direct binding to LFA-1. This is consistent with our results showing that Galectin-8 binds to the surface of B cells, independently of LFA-1, and can interact directly with the BCR. Accordingly, we observe that Galectin-8 strengthens BCR downstream signaling, particularly the PI3K pathway, which could also promote actin cytoskeleton remodeling by activating downstream targets, such as the small GTPases Rac1 and Rac2 (Arana et al., 2008; Brezski and Monroe, 2007). Noticeably, we have recently shown that the formation of the B cell immune synapse correlates with a decrease in the fraction of F-actin associated with the centrosome of B cells, a process required for B cell polarization and efficient extraction and presentation of tethered antigens (Obino et al., 2016). Whether Galectin-8 enhances B cell functions by modulating cortical and/or centrosomal pools of F-actin shall now be investigated.

As mentioned above, tethered antigens are extracted through lysosome and protease secretion when presented on rigid surfaces, whereas they are extracted through mechanical forces exerted by the motor protein Myosin II when presented on flexible surfaces such as the plasma membrane of antigen-presenting cells (Natkanski et al., 2013; Obino et al., 2017; Yuseff et al., 2011). However, stimulation of B cells in the presence of Galectin-8 did not trigger higher levels of MLC phosphorylation, an indicator of Myosin II activation (Figure S3F), suggesting that proteolytic rather than mechanical extraction of antigens is being reinforced under these conditions. Nevertheless, the absence of Myosin II activation could be due to the rigid nature of the substrate in which antigens are presented in our assay, where proteolytic-dependent extraction is favored. In this context, we cannot rule out that Galectin-8 might promote Myosin II activation when antigens are recognized on more flexible surfaces and thereby enhance their mechanical extraction. This raises the importance to determine whether co-stimulatory signals act in concert with physical cues of the environment to elicit different responses to immobilized antigens. In this regard, a recent study revealed that, in the presence the TLR9 agonist, CpG, B cells do not seem to exert pulling forces to extract antigens immobilized on plasma membrane sheets, considered flexible substrates (Akkaya et al., 2018), revealing that the mode of antigen extraction can be modulated in the presence of co-stimulatory factors. Thus, focusing on the potential cross talk between co-stimulatory molecules, such as Galectins, and mechanical cues shall provide insights on how antigen extraction and processing are regulated at the B cell synapse *in vivo*. How is the antigen extraction capacity of B cells controlled by extracellular cues in the context of lymphoid organs? Our results suggest that the presence of Galectin-8 allows prolonged interactions/attachment between B cells and antigen-presenting cells (APCs), thereby favoring the recruitment of MHC-II-containing lysosomes toward the immune synapse, which can contribute to further antigen extraction and processing. Such a mechanism can enrich the repertoire of antigenic peptides presented by B cells, even when Myosin II bypasses the need for proteolytic extraction of tethered antigens. Thus, Galectin-8 emerges as an extracellular cue that can tune B cell responses *in vivo* and in pathological situations.

Galectins can modulate the signaling capacity of immune cells by interacting directly with immune receptors at the synaptic membrane. For instance, multivalent interactions between Galectin-3 and the T cell receptor (TCR) can restrict lateral movements of this receptor at the immune synapse, thereby increasing the threshold for TCR signaling (Demetriou et al., 2001). Although Galectin-8 does not form multivalent oligomers as Galectin-3, a non-quantitative proteomic analysis of Galectin-8 binding partners in B cells revealed that Galectin-8 interacts directly with the BCR (Table S1), which was also supported by a pull-down assay showing that Galectin-8 binds to the BCR. Analogously, Galectin-9 was recently shown to interact directly with the BCR and CD45 and to suppress BCR downstream signaling by restricting the lateral mobility of the receptor and favoring its association with inhibitory molecules (Cao et al., 2018). In contrast to the effect of Galectin-9, we did not observe an inhibition of BCR signaling in the presence of Galectin-8. Moreover, we detected a higher and more sustained activation of the PI3K signaling pathway in B cells stimulated with BCR ligands plus Galectin-8 compared to the ligand alone, suggesting that B cell activation and fate are upregulated by this lectin (Saric et al., 2016). The canonical PI3K/Akt pathway also regulates lysosome tubulation triggered by LPS stimulation in macrophages and dendritic cells (Saric et al., 2016). Whether the effect of Galectin-8 on the recruitment and secretion of lysosomes at the immune synapse is regulated by the PI3K pathway and induces changes in lysosome morphology remains to be addressed. Notably, Galectin-8 alone was unable to trigger GC responses *in vivo*, nor induce BCR signaling or support antigen processing and presentation *in vitro*, suggesting that enhanced B cell activation results from the concerted action of Galectin-8

and BCR ligands. Under this perspective, it will be interesting to determine whether B cells stimulated by antigens further expose ligands that promote interactions with Galectin-8.

In addition to their extracellular activity, Galectins are also known to interact with endosomal and lysosomal compartments, where they can sense membrane damage caused by invading pathogens and, in the case of Galectin-8, also trigger antibacterial autophagy (Boyle and Randow, 2013; Thurston et al., 2012). In terms of our model, B cells isolated from Galectin-8 knockout (KO) mice did not show any defects in the polarization of the centrosome and associated lysosomes at the immune synapse; however, they did display a slightly lower capacity to extract immobilized antigens at earlier time points, compared to WT cells. A plausible explanation is that intracellular Galectin-8 could be important to maintain lysosome homeostasis as it connects lysosomes to the autophagy pathway (Boyle and Randow, 2013). Consequently, the absence of Galectin-8 can indirectly affect lysosome-associated functions, such as the degradation of immobilized antigens. Alternatively, B cells themselves might produce Galectin-8 and locally secrete this lectin at the immune synapse to promote BCR signaling in an autocrine fashion and thereby further enhance antigen extraction. Overall, our results favor a role for extracellular Galectin-8, secreted by other cell types and possibly B cells themselves, in regulating the threshold for B cell activation and response to membrane-tethered antigens

Altogether, we bring forward evidence on the role of an extracellular cue, Galectin-8, in regulating B cell responses *in vivo*. We provide the molecular basis behind its role in B cell activation by showing that Galectin-8 acts as a co-stimulator, together with BCR ligands, to promote arrest phases in B cell motility and favor the formation of a stable immune synapse (IS). At this level, Galectin-8 promotes proteolytic extraction of tethered antigens by enhancing lysosome recruitment and secretion at the immune synapse, thereby leading to efficient antigen processing and presentation.

STAR★METHODS

Detailed methods are provided in the online version of this paper and include the following:

- KEY RESOURCES TABLE
- CONTACT FOR REAGENT AND RESOURCE SHARING
- EXPERIMENTAL MODEL AND SUBJECT DETAILS
  - Mice
  - Cell lines
  - Primary cells
- METHOD DETAILS
  - Reagents and antibodies
  - RNA extraction and Quantitative RT-PCR
  - Staining of lymph node cryosections
  - Preparation of BCR-ligand-coated beads
  - Immunoblotting
  - Two-photon microscopy and cell tracking
  - *In vivo* antigen uptake
  - *In vivo* antigen presentation
  - Antigen extraction and B cell polarization
  - *In vitro* antigen presentation
  - *In vitro* synapse acidification
  - Expression of rGal8 in E.coli
  - GST Pull-down
  - Proteomics
  - B cell spreading
  - Soluble Galectin-8 binding assay
  - PhosphoFACS
- QUANTIFICATION AND STATISTICAL ANALYSIS
  - Image processing
  - *In vivo* antigen uptake
  - *In vitro* antigen extraction
  - Centrosome polarization
  - Lysosome docking and synapse acidification
  - Statistics
- DATA AND SOFTWARE AVAILABILITY
  - Proteomic analysis

SUPPLEMENTAL INFORMATION

Supplemental Information includes four figures, one table, and one video and can be found with this article online at https://doi.org/10.1016/j.celrep.2018.11.052.

ACKNOWLEDGMENTS

We acknowledge the Nikon Imaging Center at CNRS-Institut Curie and PICT-IBiSA, Institut Curie (Paris, France), a member of the France-BioImaging national research infrastructure, for support in image acquisition. We gratefully thank Hélène D. Moreau for the design of the graphical abstract. D.O. was supported by fellowships from Ecole Doctorale BioSPC, Université Paris Diderot and Université Paris Descartes, and Fondation pour la Recherche Médicale (FDT20150532056). We thank Region Ile-de-France (SESAME), Paris-Diderot University (ARS), and CNRS for funding part of the LC-MS/MS equipment. M.E. was funded by a Junior Team Leader starting grant from the Laboratory of Excellence in Research on Medication and Innovative Therapeutics (LabEx LERMIT) supported by a grant from ANR (ANR-10-LABX-33) under the program "Investissements d'Avenir" (ANR-11-IDEX-0003-01) and by an ANR @RAction starting grant (ANR-14-ACHN-0008). M.-I.Y. was supported by a research grant from FONDECYT (1141182). Funding was obtained from Association Nationale pour la Recherche (ANR-PoLyBex-12-BSV3-0014-001 to A.-M.L.-D.), the European Research Council (ERC-Strapacemi-GA 243103 to A.-M.L.-D.), ECOS (C12S02 International Research grant to M.-I.Y. and A.-M.L.-D.), and CONICYT Basal Financial Program (AFB-170005 to A.G.).

AUTHOR CONTRIBUTIONS

D.O. designed, performed, and analyzed most of the experiments, assembled figures, and participated in manuscript writing. L.F. developed and supervised two-photon microscopy experiments. O.M. assisted with cell culture and immunofluorescences and performed biochemistry experiments. J.J.S., M.L., C.O., F.D.V.B., N.G., A.C., D.L., and F.S.-M. performed immunofluorescence and immunohistochemistry experiments. C.G. and T.L. conducted the mass spectometry analysis. A.G. contributed with initial ideas, funds, reagents, and analysis tools for Galectin-8. M.E. developed and supervised mouse immunization experiments, provided SW_{HEL} mice, and performed phosphosignaling experiments. M.-I.Y. and A.S. proposed the original hypothesis and made the preliminary observations. A.-M.L.-D. and M.-I.Y. designed and supervised the overall research, funded it, and wrote the manuscript.

DECLARATION OF INTERESTS

The authors declare no competing interests.

Received: October 20, 2017
Revised: October 3, 2018
Accepted: November 13, 2018
Published: December 11, 2018

REFERENCES

Akkaya, M., Akkaya, B., Kim, A.S., Miozzo, P., Sohn, H., Pena, M., Roesler, A.S., Theall, B.P., Henke, T., Kabat, J., et al. (2018). Toll-like receptor 9 antagonizes antibody affinity maturation. Nat. Immunol. *19*, 255–266.

Anginot, A., Espeli, M., Chasson, L., Mancini, S.J., and Schiff, C. (2013). Galectin 1 modulates plasma cell homeostasis and regulates the humoral immune response. J. Immunol. *190*, 5526–5533.

Arana, E., Vehlow, A., Harwood, N.E., Vigorito, E., Henderson, R., Turner, M., Tybulewicz, V.L., and Batista, F.D. (2008). Activation of the small GTPase Rac2 via the B cell receptor regulates B cell adhesion and immunological-synapse formation. Immunity *28*, 88–99.

Batista, F.D., Iber, D., and Neuberger, M.S. (2001). B cells acquire antigen from target cells after synapse formation. Nature *411*, 489–494.

Boes, M., Cerny, J., Massol, R., Op den Brouw, M., Kirchhausen, T., Chen, J., and Ploegh, H.L. (2002). T-cell engagement of dendritic cells rapidly rearranges MHC class II transport. Nature *418*, 983–988.

Boyle, K.B., and Randow, F. (2013). The role of "eat-me" signals and autophagy cargo receptors in innate immunity. Curr. Opin. Microbiol. *16*, 339–348.

Brezski, R.J., and Monroe, J.G. (2007). B cell antigen receptor-induced Rac1 activation and Rac1-dependent spreading are impaired in transitional immature B cells due to levels of membrane cholesterol. J. Immunol. *179*, 4464–4472.

Cao, A., Alluqmani, N., Buhari, F.H.M., Wasim, L., Smith, L.K., Quaile, A.T., Shannon, M., Hakim, Z., Furmli, H., Owen, D.M., et al. (2018). Galectin-9 binds IgM-BCR to regulate B cell signaling. Nat. Commun. *9*, 3288.

Cárcamo, C., Pardo, E., Oyanadel, C., Bravo-Zehnder, M., Bull, P., Cáceres, M., Martínez, J., Massardo, L., Jacobelli, S., González, A., and Soza, A. (2006). Galectin-8 binds specific beta1 integrins and induces polarized spreading highlighted by asymmetric lamellipodia in Jurkat T cells. Exp. Cell Res. *312*, 374–386.

Carrasco, Y.R., and Batista, F.D. (2006a). B cell recognition of membrane-bound antigen: an exquisite way of sensing ligands. Curr. Opin. Immunol. *18*, 286–291.

Carrasco, Y.R., and Batista, F.D. (2006b). B-cell activation by membrane-bound antigens is facilitated by the interaction of VLA-4 with VCAM-1. EMBO J. *25*, 889–899.

Carrasco, Y.R., and Batista, F.D. (2007). B cells acquire particulate antigen in a macrophage-rich area at the boundary between the follicle and the subcapsular sinus of the lymph node. Immunity *27*, 160–171.

Carrasco, Y.R., Fleire, S.J., Cameron, T., Dustin, M.L., and Batista, F.D. (2004). LFA-1/ICAM-1 interaction lowers the threshold of B cell activation by facilitating B cell adhesion and synapse formation. Immunity *20*, 589–599.

Cattaneo, V., Tribulatti, M.V., and Campetella, O. (2011). Galectin-8 tandem-repeat structure is essential for T-cell proliferation but not for co-stimulation. Biochem. J. *434*, 153–160.

Cueni, L.N., and Detmar, M. (2009). Galectin-8 interacts with podoplanin and modulates lymphatic endothelial cell functions. Exp. Cell Res. *315*, 1715–1723.

De Silva, N.S., and Klein, U. (2015). Dynamics of B cells in germinal centres. Nat. Rev. Immunol. *15*, 137–148.

Demetriou, M., Granovsky, M., Quaggin, S., and Dennis, J.W. (2001). Negative regulation of T-cell activation and autoimmunity by Mgat5 N-glycosylation. Nature *409*, 733–739.

Diskin, S., Cao, Z., Leffler, H., and Panjwani, N. (2009). The role of integrin glycosylation in galectin-8-mediated trabecular meshwork cell adhesion and spreading. Glycobiology *19*, 29–37.

Elola, M.T., Blidner, A.G., Ferragut, F., Bracalente, C., and Rabinovich, G.A. (2015). Assembly, organization and regulation of cell-surface receptors by lectin-glycan complexes. Biochem. J. *469*, 1–16.

Eshkar Sebban, L., Ronen, D., Levartovsky, D., Elkayam, O., Caspi, D., Aamar, S., Amital, H., Rubinow, A., Golan, I., Naor, D., et al. (2007). The involvement of CD44 and its novel ligand galectin-8 in apoptotic regulation of autoimmune inflammation. J. Immunol. *179*, 1225–1235.

Fleire, S.J., Goldman, J.P., Carrasco, Y.R., Weber, M., Bray, D., and Batista, F.D. (2006). B cell ligand discrimination through a spreading and contraction response. Science *312*, 738–741.

Goodnow, C.C., Crosbie, J., Adelstein, S., Lavoie, T.B., Smith-Gill, S.J., Brink, R.A., Pritchard-Briscoe, H., Wotherspoon, J.S., Loblay, R.H., Raphael, K., et al. (1988). Altered immunoglobulin expression and functional silencing of self-reactive B lymphocytes in transgenic mice. Nature *334*, 676–682.

Harwood, N.E., and Batista, F.D. (2011). The cytoskeleton coordinates the early events of B-cell activation. Cold Spring Harb. Perspect. Biol. *3*, a002360.

Hsieh, S.H., Ying, N.W., Wu, M.H., Chiang, W.F., Hsu, C.L., Wong, T.Y., Jin, Y.T., Hong, T.M., and Chen, Y.L. (2008). Galectin-1, a novel ligand of neuropilin-1, activates VEGFR-2 signaling and modulates the migration of vascular endothelial cells. Oncogene *27*, 3746–3753.

Junt, T., Moseman, E.A., Iannacone, M., Massberg, S., Lang, P.A., Boes, M., Fink, K., Henrickson, S.E., Shayakhmetov, D.M., Di Paolo, N.C., et al. (2007). Subcapsular sinus macrophages in lymph nodes clear lymph-borne viruses and present them to antiviral B cells. Nature *450*, 110–114.

Kaltner, H., and Gabius, H.J. (2012). A toolbox of lectins for translating the sugar code: the galectin network in phylogenesis and tumors. Histol. Histopathol. *27*, 397–416.

Lankar, D., Vincent-Schneider, H., Briken, V., Yokozeki, T., Raposo, G., and Bonnerot, C. (2002). Dynamics of major histocompatibility complex class II compartments during B cell receptor-mediated cell activation. J. Exp. Med. *195*, 461–472.

Lau, K.S., Partridge, E.A., Grigorian, A., Silvescu, C.I., Reinhold, V.N., Demetriou, M., and Dennis, J.W. (2007). Complex N-glycan number and degree of branching cooperate to regulate cell proliferation and differentiation. Cell *129*, 123–134.

Le Roux, D., Lankar, D., Yuseff, M.I., Vascotto, F., Yokozeki, T., Faure-André, G., Mougneau, E., Glaichenhaus, N., Manoury, B., Bonnerot, C., and Lennon-Duménil, A.M. (2007). Syk-dependent actin dynamics regulate endocytic trafficking and processing of antigens internalized through the B-cell receptor. Mol. Biol. Cell *18*, 3451–3462.

Limon, J.J., and Fruman, D.A. (2012). Akt and mTOR in B cell activation and differentiation. Front. Immunol. *3*, 228.

Malherbe, L., Filippi, C., Julia, V., Foucras, G., Moro, M., Appel, H., Wucherpfennig, K., Guéry, J.C., and Glaichenhaus, N. (2000). Selective activation and expansion of high-affinity $CD4^+$ T cells in resistant mice upon infection with *Leishmania major*. Immunity *13*, 771–782.

Marth, J.D., and Grewal, P.K. (2008). Mammalian glycosylation in immunity. Nat. Rev. Immunol. *8*, 874–887.

Massardo, L., Metz, C., Pardo, E., Mezzano, V., Babul, M., Jarpa, E., Guzmán, A.M., André, S., Kaltner, H., Gabius, H.J., et al. (2009). Autoantibodies against galectin-8: their specificity, association with lymphopenia in systemic lupus erythematosus and detection in rheumatoid arthritis and acute inflammation. Lupus *18*, 539–546.

Mattila, P.K., Batista, F.D., and Treanor, B. (2016). Dynamics of the actin cytoskeleton mediates receptor cross talk: An emerging concept in tuning receptor signaling. J. Cell Biol. *212*, 267–280.

Natkanski, E., Lee, W.Y., Mistry, B., Casal, A., Molloy, J.E., and Tolar, P. (2013). B cells use mechanical energy to discriminate antigen affinities. Science *340*, 1587–1590.

Obino, D., and Lennon-Duménil, A.M. (2014). A critical role for cell polarity in antigen extraction, processing, and presentation by B lymphocytes. Adv. Immunol. *123*, 51–67.

Obino, D., Farina, F., Malbec, O., Sáez, P.J., Maurin, M., Gaillard, J., Dingli, F., Loew, D., Gautreau, A., Yuseff, M.I., et al. (2016). Actin nucleation at the centrosome controls lymphocyte polarity. Nat. Commun. *7*, 10969.

Obino, D., Diaz, J., Sáez, J.J., Ibañez-Vega, J., Sáez, P.J., Alamo, M., Lankar, D., and Yuseff, M.I. (2017). Vamp-7-dependent secretion at the immune synapse regulates antigen extraction and presentation in B-lymphocytes. Mol. Biol. Cell *28*, 890–897.

Pardo, E., Cárcamo, C., Uribe-San Martín, R., Ciampi, E., Segovia-Miranda, F., Curkovic-Peña, C., Montecino, F., Holmes, C., Tichauer, J.E., Acuña, E., et al. (2017). Galectin-8 as an immunosuppressor in experimental autoimmune encephalomyelitis and a target of human early prognostic antibodies in multiple sclerosis. PLoS One *12*, e0177472.

Phan, T.G., Amesbury, M., Gardam, S., Crosbie, J., Hasbold, J., Hodgkin, P.D., Basten, A., and Brink, R. (2003). B cell receptor-independent stimuli trigger immunoglobulin (Ig) class switch recombination and production of IgG autoantibodies by anergic self-reactive B cells. J. Exp. Med. *197*, 845–860.

Rabinovich, G.A., and Croci, D.O. (2012). Regulatory circuits mediated by lectin-glycan interactions in autoimmunity and cancer. Immunity *36*, 322–335.

Rabinovich, G.A., and Toscano, M.A. (2009). Turning "sweet" on immunity: galectin-glycan interactions in immune tolerance and inflammation. Nat. Rev. Immunol. *9*, 338–352.

Saez de Guinoa, J., Barrio, L., and Carrasco, Y.R. (2013). Vinculin arrests motile B cells by stabilizing integrin clustering at the immune synapse. J. Immunol. *191*, 2742–2751.

Saric, A., Hipolito, V.E., Kay, J.G., Canton, J., Antonescu, C.N., and Botelho, R.J. (2016). mTOR controls lysosome tubulation and antigen presentation in macrophages and dendritic cells. Mol. Biol. Cell *27*, 321–333.

Sarter, K., Janko, C., André, S., Muñoz, L.E., Schorn, C., Winkler, S., Rech, J., Kaltner, H., Lorenz, H.M., Schiller, M., et al. (2013). Autoantibodies against galectins are associated with antiphospholipid syndrome in patients with systemic lupus erythematosus. Glycobiology *23*, 12–22.

Schindelin, J., Arganda-Carreras, I., Frise, E., Kaynig, V., Longair, M., Pietzsch, T., Preibisch, S., Rueden, C., Saalfeld, S., Schmid, B., et al. (2012). Fiji: an open-source platform for biological-image analysis. Nat. Methods *9*, 676–682.

Segovia-Miranda, F., Serrano, F., Dyrda, A., Ampuero, E., Retamal, C., Bravo-Zehnder, M., Parodi, J., Zamorano, P., Valenzuela, D., Massardo, L., et al. (2015). Pathogenicity of lupus anti-ribosomal P antibodies: role of cross-reacting neuronal surface P antigen in glutamatergic transmission and plasticity in a mouse model. Arthritis Rheumatol. *67*, 1598–1610.

Spillane, K.M., and Tolar, P. (2017). B cell antigen extraction is regulated by physical properties of antigen-presenting cells. J. Cell Biol. *216*, 217–230.

Thurston, T.L., Wandel, M.P., von Muhlinen, N., Foeglein, A., and Randow, F. (2012). Galectin 8 targets damaged vesicles for autophagy to defend cells against bacterial invasion. Nature *482*, 414–418.

Tribulatti, M.V., Cattaneo, V., Hellman, U., Mucci, J., and Campetella, O. (2009). Galectin-8 provides costimulatory and proliferative signals to T lymphocytes. J. Leukoc. Biol. *86*, 371–380.

Tsai, C.M., Chiu, Y.K., Hsu, T.L., Lin, I.Y., Hsieh, S.L., and Lin, K.I. (2008). Galectin-1 promotes immunoglobulin production during plasma cell differentiation. J. Immunol. *181*, 4570–4579.

Tsai, C.M., Guan, C.H., Hsieh, H.W., Hsu, T.L., Tu, Z., Wu, K.J., Lin, C.H., and Lin, K.I. (2011). Galectin-1 and galectin-8 have redundant roles in promoting plasma cell formation. J. Immunol. *187*, 1643–1652.

Vascotto, F., Lankar, D., Faure-André, G., Vargas, P., Diaz, J., Le Roux, D., Yuseff, M.I., Sibarita, J.B., Boes, M., Raposo, G., et al. (2007). The actin-based motor protein myosin II regulates MHC class II trafficking and BCR-driven antigen presentation. J. Cell Biol. *176*, 1007–1019.

Vicuña, L., Pardo, E., Curkovic, C., Döger, R., Oyanadel, C., Metz, C., Massardo, L., González, A., and Soza, A. (2013). Galectin-8 binds to LFA-1, blocks its interaction with ICAM-1 and is counteracted by anti-Gal-8 autoantibodies isolated from lupus patients. Biol. Res. *46*, 275–280.

Vizcaíno, J.A., Csordas, A., del-Toro, N., Dianes, J.A., Griss, J., Lavidas, I., Mayer, G., Perez-Riverol, Y., Reisinger, F., Ternent, T., et al. (2016). 2016 update of the PRIDE database and its related tools. Nucleic Acids Res. *44* (*D1*), D447–D456.

Yamamoto, H., Nishi, N., Shoji, H., Itoh, A., Lu, L.H., Hirashima, M., and Nakamura, T. (2008). Induction of cell adhesion by galectin-8 and its target molecules in Jurkat T-cells. J. Biochem. *143*, 311–324.

Yuseff, M.I., and Lennon-Dumenil, A.M. (2013). Studying MHC class II presentation of immobilized antigen by B lymphocytes. Methods Mol. Biol. *960*, 529–543.

Yuseff, M.I., Reversat, A., Lankar, D., Diaz, J., Fanget, I., Pierobon, P., Randrian, V., Larochette, N., Vascotto, F., Desdouets, C., et al. (2011). Polarized secretion of lysosomes at the B cell synapse couples antigen extraction to processing and presentation. Immunity *35*, 361–374.

STAR★METHODS

KEY RESOURCES TABLE

REAGENT or RESOURCE	SOURCE	IDENTIFIER
Antibodies		
rabbit anti-γ-Tubulin	Abcam	Cat#Ab11317; RRID: AB_297921
rat anti-Lamp-1 (CD107a)	BD PharMingen	Cat #553792; RRID: AB_2134499
AlexaFluor647-conjugated rat anti-CD169	AbD Serotec	Cat#MCA947A647; RRID: AB_10545834
mouse anti-CD45.2-FITC	BD PharMingen	Cat#553772; RRID: AB_395041
rat anti-CD4-APC	eBioscieince	Cat#17-0041-83; RRID: AB_469321
rat anti-CD45R/B220-PE	BD PharMingen	Cat#553090; RRID: AB_394620
rat anti-CXCR5-PE-Cy7	BD PharMingen	Cat#560617; RRID: AB_1727521
hamster anti-PD1-PerCP-eFluor710	eBioscience	Cat#46-9985-82; RRID: AB_11150055
rat anti-GL7-BV421	BD Horizon	Cat#562967; RRID: AB_2737922
hamster anti-FAS-BV510	BD Horizon	Cat#563646; RRID: AB_2738345
biotinylated rabbit anti-HEL	Abcam	Cat#Ab34620; RRID: AB_776112
Streptavidin-APC-eFluor780	eBioscience	Cat#47-4317-82; RRID: AB_10366688
Anti-phospho-Myosin Light Chain (pSer19)	Sigma Aldrich	Cat#M6068; RRID: AB_262024
PE Mouse Anti-ERK1/2 (pT202/pY204)	BD Biosciences	Cat# 612566; RRID: AB_399857
Alexa Fluor® 647 Mouse Anti-ZAP70 (PY319)/Syk (PY352)	BD Biosciences	Cat#557817; RRID: AB_396884
Alexa Fluor® 488 Mouse anti-BLNK (pY84)	BD Biosciences	Cat# 558444; RRID: AB_2064951
BV421 Mouse Anti-Btk (pY223)/Itk (pY180)	BD Biosciences	Cat# 564848; RRID: AB_2738982
PE-CF594 Mouse Anti-Akt (pS473)	BD Biosciences	Cat#562465; RRID: AB_2737620
Chemicals, Peptides, and Recombinant Proteins		
CypHer5E NHS Ester	GE Healthcare	Cat#PA15401
Recombinant rat Galectin-8	Sigma-Aldrich	Cat# G3670-100UG
Recombinant HEL	Recombinant Protein platform, UMR144, Institut Curie	N/A
Recombinant ovalbumin	Sigma-Aldrich	Cat# A5503
Recombinant Lack	Recombinant Protein platform, UMR144, Institut Curie	N/A
Critical Commercial Assays		
BD optEIA Mouse IL-2 ELISA set	BD Biosciences	Cat#555148
Deposited Data		
Proteomic analysis of Galectin-8 interacting proteins	This paper	https://www.ebi.ac.uk/pride/archive/login; Project accession: PXD011522
Experimental Models: Cell Lines		
Mouse IgG^+ B lymphoma cell line IIA1.6	Lankar et al., 2002	N/A
Mouse LMR7.5 T cell hybridoma	Malherbe et al., 2000	N/A
Experimental Models: Organisms/Strains		
Mouse: *Lgals8*$^{-/-}$: C57BL/6NTac- *Lgals8*$^{tm1(KOMP)Vlcg}$	KOMP Repository	Cat#VG14305
Mouse: MD4: C57BL/6-MD4	Goodnow et al., 1988	N/A
Mouse: MHC-II-GFP: C57BL/6- I-A^bβ-GFP	Boes et al., 2002	N/A
Mouse: SW_{HEL}: C57BL/6-SW_{HEL}	Marion Espéli (Phan et al., 2003)	N/A
Oligonucleotides		
qRT-PCR primer for *Lgals8 (the exact sequence is proprietary but is included in the target sequence caagaacaaattccaggtggctgtg)*	Life Technologies	Cat#4331182_Mm01332239-m1

(*Continued on next page*)

Continued		
REAGENT or RESOURCE	SOURCE	IDENTIFIER
Software and Algorithms		
Prism 7.0d	GraphPad	https://www.graphpad.com/
Fiji (ImageJ)	Schindelin et al., 2012	https://fiji.sc/#download
Imaris	Bitplane	http://www.bitplane.com/
FlowJo v10	FlowJo, LLC	https://www.flowjo.com/
Other		
Polybead® Amino Microspheres 3.00 μm	Polyscience	Cat#17145-5
0.2 μm neutravidin red fluorescent-microspheres	Life Technologies	Custom (similar product Cat#F8774)

CONTACT FOR REAGENT AND RESOURCE SHARING

Further information and requests for resources and reagents should be directed to and will be fulfilled by the Lead Contact, María-Isabel Yuseff (myuseff@bio.puc.cl).

EXPERIMENTAL MODEL AND SUBJECT DETAILS

Mice

Sperm from *Lgals8*$^{-/-}$ mice (Mouse Project ID VG14305, *Lgals8*$^{tm1(KOMP)Vlcg}$ deleted allele) were purchased from the Knockout Mouse Project (KOMP) Repository (University of California, Davis). *Lgals8*$^{-/-}$ mice were generated by *in vitro* fertilization of C57BL/6 WT mice. *Lgals8*$^{-/-}$ mice carry a LacZ expression cassette at the *Lgals8* endogenous locus. *Lgals8*$^{-/-}$ mice were breeded with C57BL/6 CD45.1 mice to obtain *Lgals8*$^{-/-}$ CD45.1 mice. The transgenic mouse line MD4, whose B cells carry transgenic (Tg) BCR specific for Hen Egg Lysozyme (HEL) (Goodnow et al., 1988), and the IA^{b}-β-GFP genetically targeted mice (MHC-II-GFP) (Boes et al., 2002) were crossed to obtained MD4 Tg/I-A^{b}β-GFP mice. All mice were housed at Département de Cryopréservation, Distribution, Typage et Archivage animal (CDTA) (TAAM, UPS44, Orléans, France) in an accredited specific-pathogen-free animal facility except for SW$_{HEL}$ mice (Phan et al., 2003) housed in the specific-pathogen-free Animex MIPSIT facility (Clamart, France, agreement number C9202301). Experiments and sacrifices were performed in accordance with the guidelines and regulations of the French Veterinary Department and the ethical committee from the Institut Curie. Spleens from SW$_{HEL}$ mice and OT-II mice were kindly provided by Marion Espéli and Olivier Lantz (Institut Curie, Paris), respectively. For all experiments, male and female (donors) and only female (recipients) mice between 6 and 10-weeks of age were used. Littermates were randomly assigned to experimental groups.

Cell lines

The mouse IgG^{+} B lymphoma cell line IIA1.6 (derived from the A20 cell line [ATCC #: TIB-208], which derives from an old BALB/c AnN mouse [sex and precise age unknown) (Lankar et al., 2002) and the LMR7.5 T cell hybridoma (derived from a 8-12 weeks old transgenic B10.D2 mouse carrying the rearranged TCR β chain of the *Lack*-specific LMR16.2 T cell hybridoma (16.2β) [sex unknown]), which recognizes I-A^{d}-*Lack*$_{156–173}$ complexes (Malherbe et al., 2000) were cultured in CLICK medium (RPMI 1640 – GlutaMaxTM-I supplemented with 10% fetal calf serum, 1% penicillin–streptomycin, 0.1% β-mercaptoethanol and 2% sodium pyruvate) (Le Roux et al., 2007). All cell culture products were purchased from GIBCO/Life Technologies. All *in vitro* experiments were conducted in 50% CLICK / 50% RPMI 1640 – GlutaMaxTM-I. All cell lines were monthly checked for the presence of mycoplasma.

Primary cells

Wild-type (C57BL/6) or HEL-specific (MD4 or SW$_{HEL}$) resting mature IgM^{+}-IgD^{+} B cells were purified from spleens of male and female 6-10 weeks old mice as described (Vascotto et al., 2007) using mouse negative B Cell Isolation Kit (Miltenyi) according to manufacturer's instructions. OVA-specific OT-II CD4^{+} T cells were purified from spleens using mouse negative CD4^{+} T Cell Isolation Kit (Miltenyi) according to manufacturer's instructions. All primary cells were used extemporaneously.

METHOD DETAILS

Reagents and antibodies

The *Lack* antigen was produced and purified by the Recombinant Protein platform (UMR144, Institut Curie, Paris, France). *Lack* peptide (aa 156-173) was synthetized by PolyPeptide Group. LPS from *Salmonella enterica* serotype typhimurium and recombinant rat Galectin-8 were purchased from Sigma-Aldrich. Cypher5E was purchased from GE Healthcare.

The following primary antibodies were used for immunofluorescence: rabbit anti-γ-Tubulin (Abcam, #Ab11317, 1/1000), rat anti-Lamp-1 (CD107a; BD PharMingen, #553792, 1/400), polyclonal rabbit anti-OVA (1/500), AlexaFluor647-conjugated rat anti-CD169 (AbD Serotec, #MCA974A647, 1/50). The following secondary antibodies were used: Cy3-conjugated F(ab')2 donkey anti-rabbit (Jackson ImmunoResearch, 1/200) and AlexaFluor488- and 647-conjugated donkey anti-rat (Life Technologies, 1/200). 4',6-Diamidino-2-phenyindole (DAPI, Sigma Aldrich, 1/5000) was used to counterstain nuclei.

RNA extraction and Quantitative RT-PCR

RNA extraction was performed from 30 mg of tissues or $10x10^6$ cells using Nucleospin RNA kit II (Macherey Nagel) according to manufacturer's instructions. Reverse transcription was performed with 1 μg RNA using the SuperScript® VILO cDNA Synthesis Kit (Invitrogen) according to manufacturer's instructions. Galectin-8 (primer: Mm01332239-m1 *Lgals*8, Life Technologies) mRNA levels were assessed using TaqMan Gene Expression Master Mix (Applied Biosystems) according to manufacturer's recommendations. Values were normalized with respect to Gapdh expression levels. For LPS-induced systemic inflammation, C57BL/6 WT mice received one retro-orbital injection of 50, 20 or 10 μg LPS (in 200 μl 1x PBS) 6 h prior to RNA extraction.

Staining of lymph node cryosections

Lymph nodes were fixed by perfusion of 4% paraformaldehyde in PB buffer (0.1 M phosphate buffer, pH 7.4), dehydrated in 30% sucrose and serial cryosectioned in 5 μm-thick sections (except for *in vivo* antigen uptake assays for which 30 μm-thick sections were performed). Galectin-8 expression was followed by detecting β-Galactosidase activity in cells that possess an active *Lgals8* promoter, as an alternative to the use of commercial antibodies against Galectin-8, which did not provide specific staining in our hands. For β-Galactosidase staining, sections were incubated over-night at 37°C with β-Gal staining solution, according to (Segovia-Miranda et al., 2015), and when indicated later stained with 5% aqueous eosin. For histo-immunofluorescence labeling, sections were blocked with TBS/BSA/Tween20 (1x/3%/0.3%) for 20 min and incubated over-night at 4°C with primary antibodies and 60 min with secondary antibodies in TBS/BSA (1x/3%). All sections were then mounted with Entellan for imaging.

Preparation of BCR-ligand-coated beads

For *in vitro* experiments, $4x10^7$ 3 μm latex NH_2-beads (Polyscience) were activated with 8% glutaraldehyde (Sigma Aldrich) for 2 h at room temperature as previously described (Obino et al., 2016; Yuseff et al., 2011). Beads were washed with 1x PBS and incubated over-night at 4°C with different ligands: 100 μg/ml of either $F(ab')_2$ goat anti-mouse IgG or $F(ab')_2$ goat anti-mouse IgM (both from MP Biomedical) in combination or not with 100 μg/ml of either ovalbumin (OVA), the *Leishmania major* antigen *Lack* and/or 0.5 μM rGalectin-8. For *in vivo* experiments, 5 μl of 0.2 μm neutravidin red fluorescent-microspheres stock solution (Life Technologies) were washed in PBS/BSA (1x/1%) and incubated over-night with biotinylated HEL or BSA (7.5 μg and 15 μg, respectively) in combination or not with biotinylated rGalectin-8 (7.5 μg) in 500 μl PBS/BSA (1x/1%). Microspheres were washed with 1x PBS and resuspended in 125 μl 1x sterile PBS. The effective amounts of HEL immobilized on microspheres were assessed by western blotting (See *Immunoblotting* section for details).

Immunoblotting

Coated microspheres were resuspended in 1x Laemmli buffer and incubated 10 min at 95°C. Supernatants were collected and separated onto mini-PROTEAN TGX SDS-PAGE gels. Following transfer onto PVDF membranes (Trans-Blot Turbo Transfer), membranes were blocked with 5% non-fat dry milk resuspended in TBS-Tween-20 (1x/0.05%) and incubated over-night at 4°C with primary antibodies followed by 60 min incubation with secondary antibodies. Western blots were developed with Clarity Western ECL substrate and chemiluminescence was detected using the ChemiDoc imager (all from BioRad).

Two-photon microscopy and cell tracking

1 to $3x10^6$ IA^b-β-GFP-expressing MD4 (HEL-specific) or WT (HEL non-specific) B cells were adoptively transferred by retro-orbital injection (in 200 μl 1x sterile PBS) into C57BL/6 WT recipient mice 24 h prior to be immunized with indicated 0.2 μm microspheres by footpad injection (~$2x10^9$ microspheres in 25 μl, corresponding to ~1.5 μg of injected HEL). 20 min post-immunization, mice were anesthetized by *i.p.* injection of a ketamine/xylazine cocktail (100 mg/ml and 20 mg/ml, respectively. 100 μl per 20 g mouse body weight) and the popliteal lymph node draining the site of injection was prepared for two-photon imaging. The two-photon laser-scanning microscopy (TPLSM) setup used was a LSM510 Meta (Zeiss) coupled to a Maitai DeepSee femtosecond laser (690–1020 nm) (Spectra-Physics). The excitation wavelength was 900 nm. For analysis of cell motility, nine consecutive 230 × 230 μm^2 images, with 4 μm z-spacing with a 40x/1.0 NA objective (Zeiss) were taken every 30 s during 30 min. Images were average-projected, denoised (median filter, radius 2 px) with Fiji (ImageJ) software (Schindelin et al., 2012) and automatic tracking of individual cells was performed with Imaris software (Bitplane). Individual tracks were manually checked and corrected when required. 3D reconstruction shown in Figure 2B was obtained by interpolation of the brightest points.

In vivo antigen uptake

$2x10^6$ CFSE-labeled (5 μM/10^7 cells, in 1x sterile PBS, 15 min at 37°C) MD4 (HEL-specific) B cells were adoptively transferred by retro-orbital injection (in 200 μl 1x sterile PBS) into C57BL/6 WT recipient mice 24 h prior to be immunized with indicated 0.2 μm

microspheres by footpad injection (see Two-photon microscopy and cell tracking section for details). 16 h post-immunization, mice were sacrificed and the popliteal lymph nodes draining the site of injection were harvested and prepared for cryosectioning (See Staining of lymph node cryosections section for details). 90 z stack (spacing 0.35 μm) images were acquired on a confocal laser scanning TCS SP8 microscope (Leica) equipped with a 40x/1.3 NA objective (Leica). See Quantification and Statistical Analysis section for quantification details.

In vivo antigen presentation

To assess the effect of exogenous Galectin-8 on T-B cooperation *in vivo*, $2x10^6$ SW_{HEL} CD45.2 B cells and $0.5x10^6$ OT-II $CD4^+$ CD45.2 T cells were adoptively transferred by retro-orbital injection (in 200 μl sterile 1x PBS) into C57BL/6 *Lgals8*$^{+/+}$ or *Lgals8*$^{-/-}$ CD45.1 recipients. 24 h later, recipient mice were immunized by footpad injection of indicated 0.2 μm microspheres (see Two-photon microscopy and cell tracking section for details). 8 days' post-immunization, mice were sacrificed and the popliteal lymph nodes draining the site of immunization were harvested and treated with collagenase IV and DNase I for 30 min at 37°C to obtain single cell suspensions. Following Fc receptor blocking with rat anti-mouse CD16/32 antibodies (Mouse BD Fc Block, BD PharMingen), single-cell suspensions were incubated on-ice for 60 min with HEL recombinant protein (4 μg/ml) and rat anti-mouse CXCR5-PE-Cy7 (BD PharMingen, #560617, 1/50) diluted in PBS/BSA/EDTA (1x/2%/2mM). Cells were then washed and incubated on-ice for 30 min with mouse anti-mouse CD45.2-FITC (BD PharMingen, #553772), rat anti-mouse CD4-APC (eBioscieince, #17-0041-83), rat anti-mouse CD45R/B220-PE (BD PharMingen, #553090), rat anti-mouse GL7-BV421 (BD Horizon, #562967), hamster anti-mouse FAS-BV510 (BD Horizon, #563646), hamster anti-mouse PD1-PerCP-eFluor710 (eBioscience, #46-9985-82, all 1/200), biotinylated rabbit anti-HEL (Abcam, #Ab34620, 1/500) and Streptavidin-APC-eFluor780 (eBioscience, #47-4317-82, 1/100) diluted in PBS/BSA/EDTA (1x/2%/2mM). Acquisitions were performed on a FACS Verse (BD Biosciences) and data analysis was carried out with FlowJo v10.

Antigen extraction and B cell polarization

$0.25x10^6$ B lymphoma or $0.4x10^6$ spleen B cells were plated on poly-L-lysine–coated slides and stimulated with BCR-ligand$^+$ beads (cell:beads ratio: 1:2) containing OVA ± Gal8 for indicated time at 37°C, fixed in 4% PFA for 12 min at room temperature, quenched and blocked with PBS/BSA/Glycine (1x/2%/100 mM) and stained for OVA, the centrosome (γ-Tubulin) and the lysosomes (Lamp-1). For primary B cell polarization, $0.4x10^6$ spleen B cells purified from either *Lgals8*$^{+/+}$ or *Lgals8*$^{-/-}$ mice were incubated with BCR-ligand$^+$ beads containing or not Galectin-8 for indicated time, fixed and stained for the centrosome (γ-Tubulin) and lysosomes (Lamp-1). Fixed cells were incubated 45-60 min with primary antibodies and 30 min with secondary antibodies in PBS/BSA/Saponin (1x/0.2%/0.05%). Z stack (0.5 μm spacing) images of fixed cells were acquired on an inverted spinning disk confocal microscope (Roper/Nikon) with a 60x/1.4 numerical aperture (NA) oil immersion objective. See Quantification and Statistical Analysis section for quantification details.

In vitro antigen presentation

$0.1x10^6$ B lymphoma cells were incubated with BCR-ligand$^+$ beads containing *Lack* ± Gal8 for 3 h or with peptide control for 1 h. Cells were washed with 1x PBS, fixed in ice-cold Glutaraldehyde (0.01% in 1x PBS) for 1 min and quenched with Glycine (100 mM in 1x PBS). B cells were then incubated with the *Lack* specific LMR7.5 T cell hybridoma in a 1:1 ratio for 24 h. Supernatants were collected and IL-2 cytokine production was assessed using BD optEIA Mouse IL-2 ELISA set (BD Biosciences) according to the manufacturer's instructions.

In vitro synapse acidification

$0.25x10^6$ B lymphoma cells were incubated with BCR-ligand$^+$ beads containing Cypher5E ± Gal8 for 90 min. Z stack (0.5 μm spacing) images of live cells were acquired on an inverted spinning disk confocal microscope (Roper/Nikon) with a 60x/1.4 numerical aperture (NA) oil immersion objective. See Quantification and Statistical Analysis section for quantification details.

Expression of rGal8 in E.coli

Expression of recombinant GST-Gal8 was induced with 0.1 mM isopropyl-1-thio-h-digalactopyranoside (Invitrogen) for 5 h. GST-Gal8 protein was purified by affinity chromatography on glutathione-Sepharose as described by the manufacturer. The GST-Gal8 column was treated with penicillin/streptomicyn at 4°C for 16 hr. Gal8 was released from GST-Gal8 linked to glutathione–Sepharose by thrombin treatment (10 U/mg of fusion protein) for 4 h at room temperature and collected under sterile conditions. Endotoxins were eliminated using Pierce High-Capacity Endotoxin removal resin as described by the manufacturer.

GST Pull-down

$2.5x10^6$ spleen B cells were lysed for 1 h at 4°C with lysis buffer (50 mM HEPES, pH 7.4, 150 mM NaCl, 1 mM, EGTA, 2 mM MgCl2, 10% glycerol, 1% Triton X-100, 0.5 mM PMSF, 0.1 mM Pepstatin and 0.1 mM Leupeptin anti proteases) for 1 h at 4°C. The lysates were cleared by centrifugation for 10 min at 20,000 g. 300 μg of total proteins from cell extracts were incubated with 30 μl of GST-Gal8 linked to glutathione–Sepharose beads. Competence experiments were performed by pre-incubating GST-Gal8 beads with 100 mM lactose, for 1 h at 4°C. The beads were then washed in PBS, suspended and boiled in loading buffer (0.5M Tris-HCl pH 6.8, 10%

glycerol, 20% SDS, 5% beta-mercaptoethanol (v/v), 100 mM DTT, bromophenol blue). Bound BCR was resolved by 7.5% SDS-PAGE, immunoblotted onto nitrocellulose membranes with HRP-conjugated anti-mouse IgM and visualized by ECL.

Proteomics

To identify Galectin-8 interacting proteins by proteomic analysis, GST pull-down experiments were conducted as described above, except that following the incubation with B cell extracts, the GST-Gal8-beads were extensively washed in cold 1x PBS and binding partners eluted with 200 mM Lactose (1x cold PBS). Eluates were adjusted to 10 mM beta-mercaptoethanol and 0.02% SDS and denatured at 95°C for 5 min and after cooling incubated with 42 U/ml PNGase F (Sigma-Aldrich) for 2 hours at 37°C to deglycosylate the proteins. Eluted proteins were then precipitated using trichloroacetic acid (TCA), resuspended in 1x Laemmli buffer, incubated 10 min at 95°C and separated using NuPAGE Bis-Tris 4%–12% gels in MOPS buffer (Invitrogen). Gels were then stained with Coomassie blue, three plugs for each sample were cut and after destaining steps, in-gel trypsin digestion was performed. Proteins from plugs were reduced with 10 mM dithiothreitol (DTT), alkylated with 55 mM iodoacetamide (IAA) and incubated with 20 μL of 25 mM NH_4HCO_3 containing 12.5 μg/ml sequencing-grade trypsin (Promega) overnight at 37°C. Resulting digested peptides from each plug were analyzed on a Orbitrap Fusion Tribrid mass spectrometer coupled to an Easy-spray nanoelectrospray ion source and an Easy nano-LC Proxeon 1000 liquid chromatography system (all from Thermo Scientific). Chromatographic separation of the peptides was achieved by an Acclaim PepMap 100 C18 pre-column and a PepMap-RSLC Proxeon C18 column at a flow rate of 300 nl/min. The solvent gradient consisted of 95% solvent A (water, 0.1% (v/v) formic acid) to 35% solvent B (100% acetonitrile, 0.1% (v/v) formic acid) over 98 minutes for a total gradient time of 2 hours. The orbitrap cell analyzed the peptides in full ion scan mode, with the resolution set at 120 000 with a *m/z* range of 350 - 1550. Higher-energy collisional dissociation (HCD) activation with a collisional energy of 28% was used for peptide fragmentation with a quadruple isolation width of 1.6 Da. The linear ion trap was employed in top-speed mode in order to acquire the MS/MS data. Maximum ion accumulation times were set to 250 ms for MS acquisition and 60 ms for MS/MS acquisition in parallelization mode. For the identification step, all MS and MS/MS data were processed with the Proteome Discoverer software (Thermo Scientific, version 1.4) and with an in-house Mascot search engine (Matrix Science, version 2.5.1). The mass tolerance was set to 7 ppm for precursor ions and 0.5 Da for fragments. The following modifications were allowed: oxidation (M), carbamidomethylation (Cys), phosphorylation (Ser, Thr, Tyr), acetylation (N-term of protein), deamidation (Asn, Gln). The SwissProt database (10/2014) with the *Mus musculus* taxonomy was used to identify proteins. Peptide FDR (False Discovery Rate) were calculated with the Percolator algorithm. Protein were considered as identified if their mascot scores were above 50 and if more than 2 peptides per protein were identified.

B cell spreading

B lymphoma cells were seeded on coverslips coated with poly-L-lysine or 20 μg Galectin-8 for indicated time, fixed with 4% PFA for 10 min and stained with Alexa-Fluor488-conjugated Phalloidin. To assess the glycan specificity binding of Galectin-8, B cells were plated on indicated coverslips in presence of 100 mM sucrose or lactose for 60 min. To assess the dependency of Galectin-8 binding to B cell surface LFA-1, B cells were pre-treated with 10 μg/ml of function-blocking anti-LFA-1 antibody (Biolegend, #101109) before being plated on indicated coverslips for 60 min. Z stack (0.5 μm spacing) images of fixed cells were acquired on an inverted spinning disk confocal microscope (Roper/Nikon) with a 60x/1.4 numerical aperture (NA) oil immersion objective.

Soluble Galectin-8 binding assay

Recombinant Galectin-8 was coupled to AlexaFluor488 using AlexaFluor488-microscale protein labeling kit (Invitrogen, #A30006) according to manufacturer's instructions. 20 μg of AlexaFluor488-conjugated Galectin-8 (Gal8-488) were pre-treated with 20 mM of either sucrose, lactose (Sigma-Aldrich) or thiodigalactoside (TDG) (Carbosynth, Batch# OS043971301) for 30 min, then incubated with B cells for 60 min, washed and the cell-bound fraction of Gal8-488 detected by flow cytometry. A similar approach was used to assess the dependency of Galectin-8 binding to B cell surface LFA-1. In these conditions, B cells were pre-treated for 30 min with 2 μg/ml of soluble recombinant ICAM-1-Fc (Biolegend, #553004) or 10 μg/ml of function-blocking anti-LFA-1 antibody (Biolegend, #101109) to prevent the potential interaction of Galectin-8 with LFA-1 prior to be incubated for 60 min with Gal8-488.

PhosphoFACS

$1x10^6$ spleen B cells were incubated on-ice in RPMI 1640 – GlutaMaxTM-I (without serum) for 30 min prior to be stimulated with BCR-ligand$^+$ beads (cell:bead ratio 1:1) containing or not Galectin-8 for indicated time. Cells were washed in ice-cold 1x TBS, fixed with ice-cold methanol for 30 min on ice. Cells were stained with either a rabbit anti-phospho-Myosin Light Chain (pSer19) antibody followed by an AlexaFluor647-conjugated goat anti-rabbit antibody (#A21244, Invitrogen) or with a PE-conjugated anti-ERK1/2 (pT202/pY204), AlexaFluor647-conjugated anti-ZAP70 (pY319)/Syk (pY352), AlexaFluor488-conjugated anti-BLNK (pY84), BV421-conjugated anti-Btk (pY223)/Itk (pY180) and PE-CF594-conjugated anti-Akt (pS473) in TBS/BSA (1x/2%) for 45 min at room temperature, washed twice in 1x TBS. The acquisitions were performed on a Fortessa flow cytometer (BD Biosciences) and analysis were carried out with FlowJo v10.

QUANTIFICATION AND STATISTICAL ANALYSIS

Image processing

Image processing was performed with Fiji (ImageJ) software (Schindelin et al., 2012), except when mentioned. Images shown in the figures were cropped from large fields, rotated and their contrast and brightness manually adjusted.

In vivo antigen uptake

The percentage of antigen-loaded B cells was determined by manual counting of green cells (CFSE-labeled HEL-specific B cells) having internalized at least one red microsphere, as determined by the inclusion of the red fluorescent signal within the green one in 3D-reconstructed images. Then, the distribution of the number of microspheres per B cells among antigen-loaded B cells was manually assessed per each condition.

In vitro antigen extraction

The amounts of OVA (fluorescence intensity) remaining on beads at indicated time were quantified and normalized with respect to the initial OVA fluorescence intensity (t = 0 min, 100%). Results are presented as the percentage of antigen extraction calculated as 100% - % of OVA on bead. Bar graphs show the mean ± sem.

Centrosome polarization

Centrosome polarity indexes were computed as described (Obino et al., 2016). Briefly, z stacks were projected (SUM slice) and images were manually thresholded (Default) to obtain the center of mass of the cell (CellCM). Then, the position of the centrosome and the bead geometrical center (BeadGC) were manually selected. The position of the centrosome was then projected (Centproj) on the vector defined by the CellCM–BeadGC axis. The centrosome polarity index was calculated by dividing the distance between the CellCM and the Centproj by the distance between the CellCM and the BeadGC. The index ranges from -1 (anti-polarized) to 1 (fully polarized). Results are either directly displayed as the centrosome polarity index, or as the percentage of cells with a polarized centrosome (polarity index $\geq$ 0.6). Boxes in boxplots extend from the 25th to 75th percentile, with a line at the median and whiskers extend from the 10th to the 90th percentile. Bar graphs show the mean ± sem.

Lysosome docking and synapse acidification

Lamp-1^{+}-rings were manually counted. Cypher5E fluorescence signal was measured on cell-bead conjugates and normalized with respect to the mean fluorescence of beads that were not engaged in immune synapses. Bar graphs show the mean ± sem.

Statistics

All graphs and statistical analysis were performed with GraphPad Prism 7. No statistical method was used to predetermine sample size. Kolmogorov–Smirnov test was used to assess normality of all datasets. Mann-Whitney test was used to determine statistical significance excepted when mentioned. Boxes in boxplots extend from the 25th to 75th percentile, with a line at the median and whiskers extend from the 10th to the 90th percentile. Bar graphs show the mean ± sem. Statistical details of experiments (sample size, replicate number, statistical significance) can be found in the figures and figure legends.

DATA AND SOFTWARE AVAILABILITY

Proteomic analysis

The complete datasets are available in the PRIDE partner repository (Vizcaíno et al., 2016) under the identification number: PXD011522 as *.raw* files, Proteome Discoverer 1.4 *.msf* files and associated *pep.xml* and *xlsx* files.

Cell Reports, Volume *25*

Supplemental Information

Galectin-8 Favors the Presentation of Surface-Tethered Antigens by Stabilizing the B Cell Immune Synapse

Dorian Obino, Luc Fetler, Andrea Soza, Odile Malbec, Juan José Saez, Mariana Labarca, Claudia Oyanadel, Felipe Del Valle Batalla, Nicolas Goles, Aleksandra Chikina, Danielle Lankar, Fabián Segovia-Miranda, Camille Garcia, Thibaut Léger, Alfonso Gonzalez, Marion Espéli, Ana-Maria Lennon-Duménil, and Maria-Isabel Yuseff

SUPPLEMENTAL FIGURES

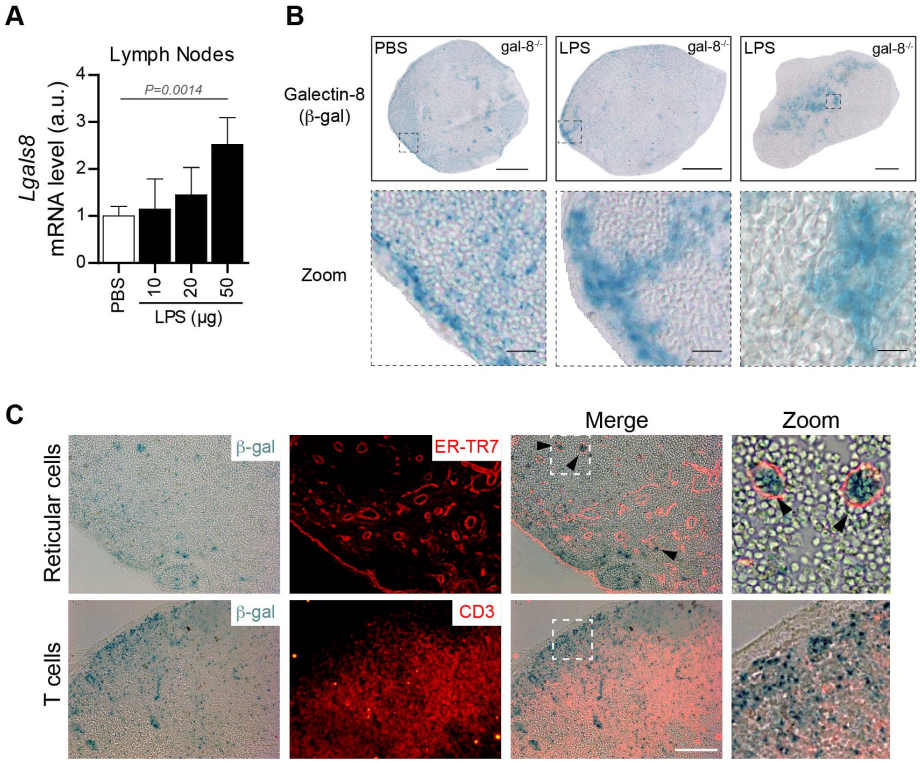

Figure S1. Galectin-8 is expressed in lymphoid tissues. Related to Figure 1. (A) Quantitative RT-PCR analysis of *Lgals8* mRNA levels in peripheral lymph nodes of C57BL/6 mice 6h following retro-orbital injection of PBS (vehicle control) or indicated doses of LPS. Values were normalized with respect to the mean PBS value per replicate. n=3 to 5 mice per condition pooled from N=4 independent experiments. Analysis of variance (ANOVA test) was used to assess statistical significance. **(B)** Representative images of β-galactosidase staining of LN cryosections from mice bearing a LacZ expression cassette at the *Lgals8* locus 6h following injection of PBS (vehicle control) or LPS (50 µg) in the tail vein. Scale bar, 500µm. Zooms highlight the increase in β-galactosidase staining within different areas upon inflammation. Scale bar, 50µm. **(C)** Representative images of popliteal lymph node sequential cryosections from mice bearing a LacZ expression cassette at the *Lgals8* locus stained for β-galactosidase (blue) and either reticular cells (ER-TR7) or T cells (CD3), both shown in red. Scale bar, 200 µm. Arrowheads highlight β-galactosidase staining within the vasculature.

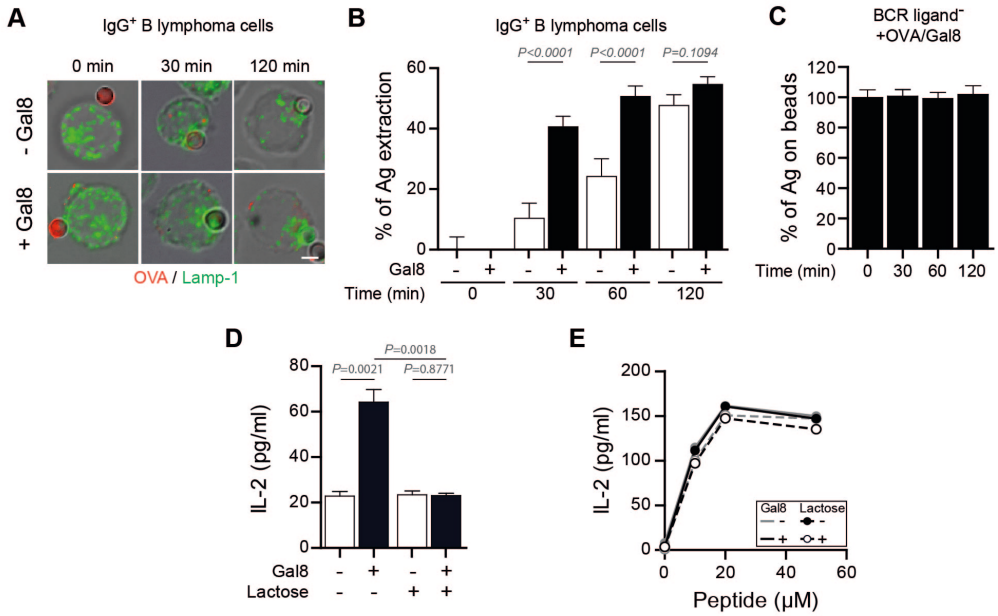

Figure S2. Galectin-8 promotes efficient antigen extraction and presentation by B lymphoma cells *in vitro*. Related to Figure 5. **(A)** Representative images of B lymphoma cells incubated with BCR-ligand^{+} beads plus the model antigen OVA in the presence or not of Galectin-8 for indicated time. Scale bar, 3 μm. **(B)** Quantification of the percentatge of antigen (OVA) extracted from beads following incubation of B lymphoma cells with BCR-ligand^{+} beads plus OVA in the presence or not of Galectin-8 for indicated time. Values were normalized with respect to Ag-coated beads not engaged with B cells. n>40 cells pooled from N=3 independent experiments. **(C)** Quantification of the amounts of antigen (OVA) remaining on beads following incubation of B lymphoma with BCR-ligand^{-} beads plus OVA/Gal8 for indicated time. n>20 cells pooled from 2 independent experiments. **(D)** Antigen presentation assay of B lymphoma cells stimulated with BCR-ligand^{+} beads containing Lack±Gal8 in the presence or not of 100 mM lactose. Data represent the mean±SEM of triplicate and are representative of N=3 independent experiments. Unpaired t-test. **(E)** Peptide control for cells used in the antigen presentation assay shown in (D). Graph shows the mean of duplicates and is representative of 3 independent experiments.

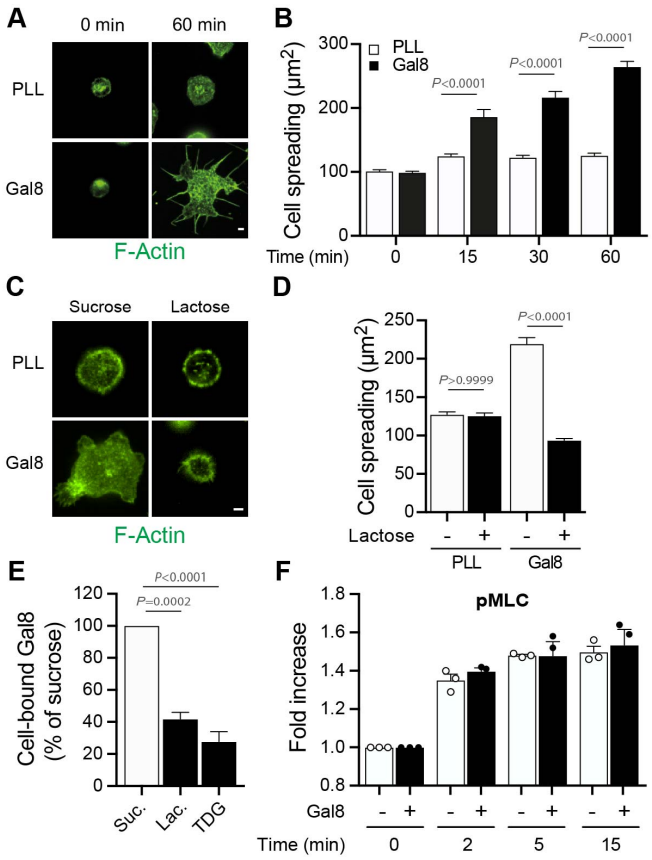

Figure S3. Galectin-8 enhances B cell spreading but not contractility. Related to Figure 5. (A) Representative images of B lymphoma cells seeded on coverslips coated with poly-L-lysine (PLL) or 20 µg Galectin-8 (Gal8) for indicated time and stained for F-Actin (Phalloidin, green) . Scale bar, 3 µm. **(B)** Quantification of the spreading area of cells shown in (A). n>90 cells pooled from N=3 independent experiments. **(C)** Representative images of B lymphoma cells seeded on coverslips coated with poly-L-lysine (PLL) or 20 µg Galectin-8 (Gal8) in presence of 100 mM sucrose (control) or lactose for 60 min and stained for F-Actin (Phalloidin, green) . Scale bar, 3 µm. **(D)** Quantification of the spreading area of cells shown in (C). n>50 cells pooled from N=2 independent experiments. **(E)** AlexaFluor488-conjugated recombinant Galectin-8 was pre-traeted with 20 mM sucrose (Suc.), lactose (Lac.) or thiodigalactoside (TDG) for 30 min prior to be incubated with B lymphoma cells for 60 min, washed and the cell-bound fraction of AlexaFluor488-Gal8 detected by flow cytometry. Values were normalized with respect to the sucrose condition in each experimental replicate. Data are pooled from N=3 independent experiments. **(F)** Flow cytometry analysis of the phosphorylation status of Myosin Regulatory Light Chain (pMLC) upon stimulation of B lymphoma cells with BCR-ligand^{+} beads containing or not Galectin-8 for indicated times. Values were normalized with respect to the time 0 min per condition and experimental replicate. Data are pooled from N=3 independent experiments. An analysis of variance (ANOVA test) followed by a Sidak's multiple comparaison test **(B, D-E)** and a ratio paired t-test **(F)** were used to assess statistical significance.

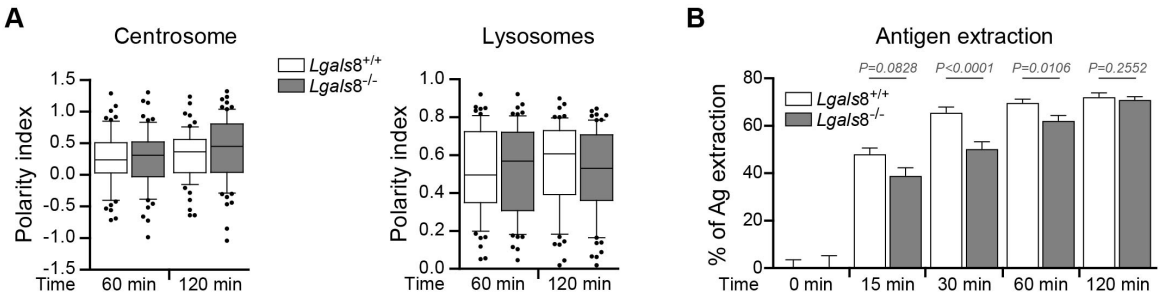

Figure S4. The lack of Galectin-8 does not impair B cell polarization and function. Related to Figure 5. (A) Quantification of centrosome and lysosome polarity indexes of spleen B cells purified from *Lgals8* $^{+/+}$ (white) and *Lgals8* $^{-/-}$ (grey) mice and stimulated for 60 min or 120 min with BCR-ligand^{+} beads. n>60 cells per condition and time point and are pooled from N=2 independent experiments. Unpaired t-test (centrosome) and Mann-Whitney test (lysosomes) were used to assess statistical significance. **(B)** Antigen (OVA) extraction assay with *Lgals8* $^{+/+}$ (white) and *Lgals8* $^{-/-}$ (grey) spleen B cells stimulated with BCR-ligand^{+} beads containing OVA for indicated time. Bars show the mean±SEM with n>55 cells per condition and time point pooled from N=2 independent experiments. Mann-Whitney test was used to assess statistical significance.